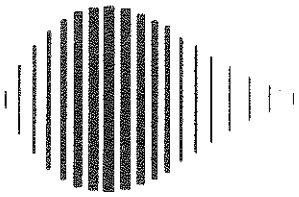

NATIONAL CENTER FOR EARTHQUAKE
ENGINEERING RESEARCH
State University of New York at Buffalo

SEISMIC RESPONSE OF PILE FOUNDATIONS

by

S.M. Mamoon, P.K. Banerjee and S. Ahmad
Department of Civil Engineering
State University of New York at Buffalo
Buffalo, New York 14260

Technical Report NCEER-88-0034

November 1, 1988

This research was conducted at the State University of New York at Buffalo and was partially supported by the National Science Foundation under Grant No. ECE 86-07591.

NOTICE

This report was prepared by the State University of New York at Buffalo as a result of research sponsored by the National Center for Earthquake Engineering Research (NCEER) and the National Science Foundation. Neither NCEER, associates of NCEER, its sponsors, State University of New York at Buffalo, nor any person acting on their behalf:

a. makes any warranty, express or implied, with respect to the use of any information, apparatus, method, or process disclosed in this report or that such use may not infringe upon privately owned rights; or

b. assumes any liabilities of whatsoever kind with respect to the use of, or the damage resulting from the use of, any information, apparatus, method or process disclosed in this report.

SEISMIC RESPONSE OF PILE FOUNDATIONS

by

S.M. Mamoon[1], P.K. Banerjee[2] and S. Ahmad[3]

November 1, 1988

Technical Report NCEER-88-0034

NCEER Contract Number 87-1013

NSF Master Contract Number ECE 86-07591

1 Graduate Student, Department of Civil Engineering, State University of New York at Buffalo
2 Professor, Department of Civil Engineering, State University of New York at Buffalo
3 Assistant Professor, Department of Civil Engineering, State University of New York at Buffalo

NATIONAL CENTER FOR EARTHQUAKE ENGINEERING RESEARCH
State University of New York at Buffalo
Red Jacket Quadrangle, Buffalo, NY 14261

PREFACE

The National Center for Earthquake Engineering Research (NCEER) is devoted to the expansion and dissemination of knowledge about earthquakes, the improvement of earthquake-resistant design, and the implementation of seismic hazard mitigation procedures to minimize loss of lives and property. The emphasis is on structures and lifelines that are found in zones of moderate to high seismicity throughout the United States.

NCEER's research is being carried out in an integrated and coordinated manner following a structured program. The current research program comprises four main areas:

- Existing and New Structures
- Secondary and Protective Systems
- Lifeline Systems
- Disaster Research and Planning

This technical report pertains to Program 1, Existing and New Structures, and more specifically to geotechnical studies, soils and soil-structure interaction.

The long term goal of research in Existing and New Structures is to develop seismic hazard mitigation procedures through rational probabilistic risk assessment for damage or collapse of structures, mainly existing buildings, in regions of moderate to high seismicity. The work relies on improved definitions of seismicity and site response, experimental and analytical evaluations of systems response, and more accurate assessment of risk factors. This technology will be incorporated in expert systems tools and improved code formats for existing and new structures. Methods of retrofit will also be developed. When this work is completed, it should be possible to characterize and quantify societal impact of seismic risk in various geographical regions and large municipalities. Toward this goal, the program has been divided into five components, as shown in the figure below:

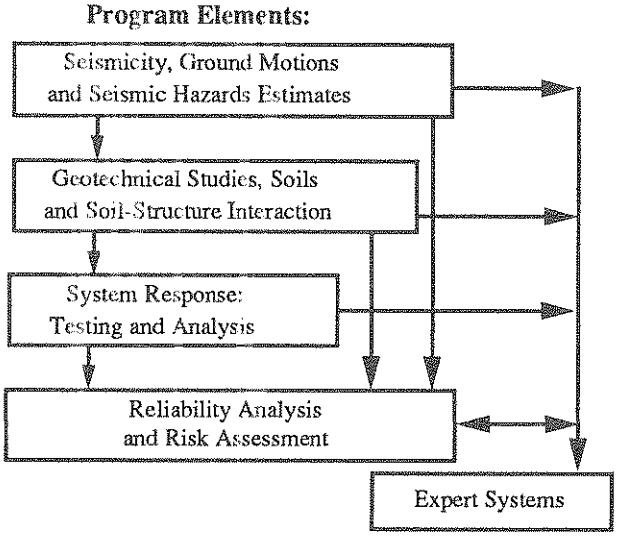

Geotechnical studies, soil and soil-structure interaction constitute one of the important areas of research in Existing and New Structures. Current research activities include the following:

1. Development of linear and nonlinear site response estimates.
2. Development of liquefaction and large ground deformation estimates.
3. Investigation of soil-structure interaction phenomena.
4. Development of computational methods.
5. Incorporation of local soil effects and soil-structure interaction into existing codes.

The ultimate goal of projects in this area is to develop methods of engineering estimation of large soil deformations, site response, and the effect that the interaction of structures and soils have on the resistance of structures against earthquakes.

Increasing numbers of structures and buildings are built on poorly performing soils which require pilings for stability. Thus, the understanding of the performance of piling in soft soils under dynamic loads is of increasing importance. This paper addresses fundamental methods to analytically describe the behavior of a single element of a pile foundation during seismic loads. It addresses but one element in a complex problem which needs to be solved step by step to devise methods to increase the earthquake resistance of new and existing structures, many of which require pile foundations. Thus, this study must be seen as one step in a sequence of investigations carried out by NCEER in the field of soil-structure interaction.

ABSTRACT

A boundary element formulation is presented to analyze the seismic response of a single pile. The piles are modeled by compressible beam-column elements and the soil as a hysteretic elastic half-space. A new Green's function corresponding to dynamic loads in the interior of a semi-infinite solid is developed for this study. The governing differential equations of motion for the pile domain have been solved exactly for distributed periodic loading intensities. These solutions were then coupled with a numerical solution for the motion of the soil domain by satisfying equilibrium and compatibility at the pile-soil interface. The responses were evaluated over wide ranges of the parameters involved to vertically and obliquely incident P, SV and SH-waves. Results are presented as dimensionless graphs and the pile-soil interaction is studied. It is observed that the existence of the pile produces a filtering of the waves, reducing the amplitude of motion as a function of frequency. Also the filtering effects, the pile motions and the amplitudes are found to be dependent on the slenderness ratio, the stiffness ratio and the angle of incidence. Finally, an actual transient analysis is performed to study the response of piles to seismic waves in the time domain.

ACKNOWLEDGEMENT

The work presented in this report was made possible by NCEER Grant No. 87-1013 from the National Center for Earthquake Engineering Research, State University of New York at Buffalo. This support is gratefully acknowledged. The computations were performed on an HP 9000 series computer that belongs to the Computational Mechanics Division, Department of Civil Engineering, State University of New York at Buffalo.

TABLE OF CONTENTS

LIST OF FIGURES

SECTION 1

INTRODUCTION

In recent years much progress has been made in developing procedures for calculating the responses of single piles and pile groups to both static [4,5,7,19] and dynamic loads [6,7,13,20,21]. However, realistic dynamic analyses of pile foundations have received comparatively less attention; most of the work done is essentially restricted to foundations subjected to periodic excitations [6,7,13,20,21]. It is well known that the excitation in an actual earthquake is a complex time dependent function and therefore, in order to predict the seismic response of pile foundations, it is necessary to carry out a transient analysis [12].

The effect of vertically and obliquely incident seismic waves on surface and embedded shallow foundations has been investigated in some detail in recent years [9,22]. Simplified rules have been suggested [9,22] to estimate both the translational and rotational response from the free-field motion as a function of the embedment depth. It was found that the existence of the foundation produces a filtering of the waves, reducing the amplitude of the motion as a function of frequency.

However, relatively few reports exist in the published literature with regard to the behavior of deep foundations (piles, piers and caissons) to traveling waves. The response of piles to vertically propagating S-waves has been studied by several authors [11,12]. Gazetas [12] has presented results of a numerical study of the dynamic response of end-bearing piles embedded in a number of idealized soil deposits. Still, several questions remain unanswered, especially with regard to the practical assessment of the influence of piles on the seismic excitation of a structure. Furthermore, only a very limited number of results are available in the form of dimensionless graphs [16].

It is the objective of this report to present the results of a study on the behavior of a single pile subjected to incident P, SV and SH-waves. Such results would be useful not only for developing an improved understanding of the mechanics of the problem, but, also for deriving simple preliminary design rules for foundation engineering practice. Such a study is well worth undertaking, since the majority of important structures, such as tall buildings, major highway bridges, offshore oil platforms, etc., are supported on piled foundations and the existing state of knowledge is poor. Also, the results would be of great interest to many engineers who have built heavy structures on soft soils in seismic prone areas.

In the present work, the modeling of this problem has been done by means of a hybrid boundary element formulation [3]. The numerical scheme is based on the discretization of the pile and the soil domain around the pile into elements throughout which the displacement and tractions are assumed to be constant (or can be interpolated between nodal values in a higher order formulation). The boundary element method offers considerable advantage over the other numerical methods, for this problem, primarily because of its ability to take into account the three dimensional effects of soil continuity and boundaries at infinity. In this work, for soil-domain a new fundamental solution corresponding to a periodic dynamic point force in the interior of an elastic half-space is developed and then used in the numerical scheme. This solution represents the dynamic equivalent of Mindlin's [18] static half-space point force solution.

SECTION 2

METHOD OF ANALYSIS

2.1 GOVERNING EQUATIONS

The general strategy used for the analysis of the pile foundations under static and dynamic loading by Banerjee and Driscoll [5], Sen et al [20,21] is followed here. This involves the construction of an integral representation for the soil domain and the equations of motion for the piles, represented by linear structural components.

For dynamic loading of a homogeneous, isotropic, elastic solid, the governing differential equation in terms of the displacements u_i (neglecting body forces) is [3]:

$$(\lambda+\mu)u_{j,ji} + \mu u_{j,ji} - \rho\ddot{u}_i = 0 \tag{2.1}$$

where

λ, μ are the Lame's constant

ρ is the mass density of the solid

$\ddot{u}_i = \partial^2 u_i/\partial t^2$ are the accelerations

If the displacements are periodic (time harmonic), i.e.,

$$u_i(x,t) = u_i(x,\omega)e^{i\omega t} \tag{2.2}$$

where $u_i(x,\omega)$ is the amplitude of the displacement and ω is the circular frequency, then, equation (2.1) reduces to Helmholtz's equation [3]

$$(\lambda+\mu)u_{j,ji} + \mu u_{i,jj} + \rho\omega^2 u_i = 0 \tag{2.3}$$

For a homogeneous solid of finite extent the solution of this differential equation for arbitrary boundary conditions can be expressed as an integral equation in which the full-space Green's function takes the roles of the kernel function [3]. However, in the present application, in

which the solid is of semi-infinite extent, it is advantageous to cast the integral equation in terms of the Green's function for the half-space, since this reduces the domain of integration to the soil-pile interface only. The integral equation describing the motion of the soil can be written as:

$$u_j(\xi,\omega) = \int_S G_{ij}(x,\xi,\omega)\phi_i(x,\omega)ds \qquad (2.4)$$

where

u_j are the displacements of the soil

G_{ij} is the Green's function for an elastic, homogeneous half-space

ϕ_i are the tractions at the pile soil interface

Equation (2.4) must be coupled with equations describing the response of the piles (idealized as beam-column structures) to axial and flexural harmonic excitations. The equations of motion [20] are:

$$m\omega^2 u_z + E_p A_p \frac{d^2 u_z}{dz^2} = -\pi d\phi_z \qquad (2.5)$$

for the axial dynamic response and

$$E_p I_p \frac{\partial^4 u_x}{\partial z^4} + m\frac{\partial^2 u_x}{\partial t^2} = -d\phi_x \qquad (2.6)$$

for the lateral dynamic response, where

E_p the Young's modulus of the pile material

I_p the second moment of the area of pile cross-section

A_p the cross sectional area of the pile shaft

d the diameter of the pile

u_x and u_z are the lateral and axial displacements, respectively

m the mass per unit length of the pile

ϕ_x and ϕ_z are the lateral and axial tractions on the pile

Equations (2.4), (2.5) and (2.6) represent the complete set of equations for the solution of the problem.

2.2 NUMERICAL SOLUTION

By discretizing the pile-shaft-soil interfaces into n cylindrical segments, the bases of the piles being circular discs, we can use equation (2.4) to determine the displacements at the pile-soil interface as

$$u_j(\xi_m,\omega) = \sum_{p=1}^{n} [\int_{\Delta S_p} G_{ij}(x,\xi_m,\omega) dS_p] \phi_i^p(x,\omega) \qquad (2.7)$$

where surface tractions ϕ_i^p have been assumed to be constant over each segment of the pile-shaft soil and pile-base soil interfaces p(p=1,...,n).

By taking ξ_m successively as the centroidal point of each element on the boundary, we can obtain the following matrix equations for the interfaces:

$$\{u_s^s\} = [G]\{\phi_s^s\} \qquad (2.8)$$

where superscript 's' represents the scattered values and the subscript 's' indicates that the stress and displacement values are obtained from a consideration of soil domain alone.

The differential equation (2.3), the Helmholtz's equation, is that governing time harmonic wave scattering. Scattering problems dealing with

infinite and semi-infinite regions are usually formulated decomposing the total displacement and stress fields (u^t, ϕ^t) into two parts [3]: (1) a known free or undisturbed field (u^f, ϕ^f), and (2) the scattered field (u^s, ϕ^s), i.e.,

$$\{u^t\} = \{u^f\} + \{u^s\}$$
$$\{\phi^t\} = \{\phi^f\} + \{\phi^s\} \qquad (2\text{-}9)$$

The free-field or the incident wave is simply the wave motion that would be present in the absence of scattering surfaces and the scattered part is the wave diverging from the scattering region. u^s satisfies the radiation condition at infinity, which guarantees the absence of reflected radiation.

Writing (2.8) in terms of eq. (2.9),

$$\{u_s^t\} - \{u_s^f\} = [G](\{\phi_s^t\} - \{\phi_s^f\})$$

or

$$\{u_s^t\} = [G]\{\phi_s^t\} - \{b_s\} \qquad (2.10)$$

where,

$$\{b_s\} = [G]\{\phi_s^f\} - \{u_s^f\} \; . \qquad (2.11)$$

The set of equations represented by eq. (2.10) has to be coupled with an equivalent set for the pile domain by solving the governing differential equations (2.5) and (2.6) describing the responses of the piles to axial and flexural harmonic excitation. The general solutions of these equations [i.e., (2.5) and (2.6)] are of the form [20].

$$u_z = A_1 \sin(\gamma z) + A_2 \cos(\gamma z) \qquad (2.12)$$

$$u_x = B_1 \sin(\eta z) + B_2 \cos(\eta z) + B_3 \sinh(\eta z) + B_4 \cosh(\eta z) \qquad (2.13)$$

where

$$\gamma = [m\omega^2/E_pA_p]^{1/2} \tag{2.13a}$$

$$\eta = [m\omega^2/E_pI_p]^{1/4} \tag{2.13b}$$

and the arbitrary constants can be determined from the specified boundary conditions at the ends of the pile. Since the distribution of tractions along the pile-soil interface is a complex function of nodal values of traction, direct determination of the particular solutions of equations (2.5) and (2.6) is scarcely possible. For arbitrary pile head displacements it is necessary to examine the behavior of individual piles when subjected to axial and lateral dynamic loads. This can be best done by considering the effects of applied pile head displacements as the algebraic sum of the motion of an unsupported pile (i.e., no soil reaction) under arbitrary pile head boundary conditions and those of a fixed head pile. Superposition of these solutions leads to the linear set

$$\{u_p^t\} = [D]\{\phi_p^t\} + u_1\{b_p\} \tag{2.14}$$

where $\{b_p\}$ is the displacement vector derived from unit pile-head boundary conditions, the matrix [D] comprises constants of equations (2.12) and (2.13), and u_1 is the arbitrary pile head displacements or rotation. Here 't' indicates the total field values and subscript 'p' indicates that the pile-soil interface displacements and tractions are obtained from a consideration of pile domain alone. Equation (2.14) may be rearranged into,

$$[B]\{u_p^t\} = [D]\{\phi_p^t\} \tag{2.15}$$

where [B] is an identity matrix with $\{b_p\}$ vector subtracted out from the first column for the axial case. The corresponding $\{b_p\}$ vector is similarly incorporated in the first column for the lateral case.

Now premultiplying both sides of equation (2.10) with [B] matrix we have

$$[B]\{u_s^t\} = [B][G]\{\phi_s^t\} - [B]\{b_s\} = [E]\{\phi_s^t\} - \{d_s\} \tag{2.16}$$

where, $$[E] = [B][G] \tag{2.17}$$

and, $$\{d_s\} = [B]\{b_s\} \tag{2.18}$$

By satisfying the equilibrium and compatibility conditions at the pile-soil interface, the total tractions acting on the piles may be determined from (2.15) and (2.16) as

$$\{\phi_p^t\} = -\left[[D] + [E]\right]^{-1}\{d_s\} \tag{2.19}$$

The total displacements are then obtained from (2.10).

The axial loads, shear forces and bending moments in the piles at any depth due to the seismic forces can then be easily recovered from the values of ϕ_p^t and the inertial forces:

$$P_z(z) = \int_L^z [\phi_z^t \pi d + \bar{m}\omega^2 u_z^t]dz + A_b\phi_b^t \tag{2.20a}$$

$$P_x(z) = \int_L^z [\phi_x^t d + \bar{m}\omega^2 u_x^t]dz \tag{2.20b}$$

$$M(z) = \int_L^z [\phi_x^t d + \bar{m}\omega^2 u_x^t]zdz \tag{2.20c}$$

where $\bar{m}$ is the difference of mass/unit length between the pile and the soil filled pile domain.

In equation (2.11) information is needed about the free-field stress and displacement values $\{\phi_s^f\}$, $\{u_s^f\}$, which is discussed in the next section.

2.3 INCIDENT WAVES

Consider the half space $z \geq 0$ (Fig. 2-1), and a train of plane waves, propagating parallel to the x-z plane. The motions are therefore independent of the coordinate y and the overall problem can be studied in two uncoupled parts, one corresponding to SH-waves with a motion in the y-direction and the other to SV and P waves with coupled motion in the x and z-directions. The solutions adopted for SH, SV and P waves is the one obtained by direct integration of the differential equations of motion in terms of amplitudes used in reference [17], as opposed to solutions in terms of potentials proposed by some researchers [9].

SH-Waves: To be consistent with the previous formulation, we may consider the SH-waves to have a motion in the x-direction as a result of waves propagating parallel to the y-z plane. The motion for an elastic medium with one-dimensional geometry in the case of SH-waves has the form [9]:

$$u_x = [A_{SH}\exp(\frac{i\omega}{C_s} nz) + A'_{SH}\exp(-\frac{i\omega}{C_s} nz)] \cdot f(x,t) \qquad (2.21)$$

where,

ω is the angular frequency

A_{SH} and A'_{SH} are amplitudes of the incident and reflected waves

C_s is the shear wave velocity of the soil

l and n are direction cosines of direction of propagation

For the half-space, $A_{SH} = A'_{SH}$ and for a unit amplitude of the motion on the surface, eq. (2.21) reduces to [9]:

$$u_x = \cos(\frac{\omega}{C_s} nz) \cdot f(x,t) \qquad (2.22)$$

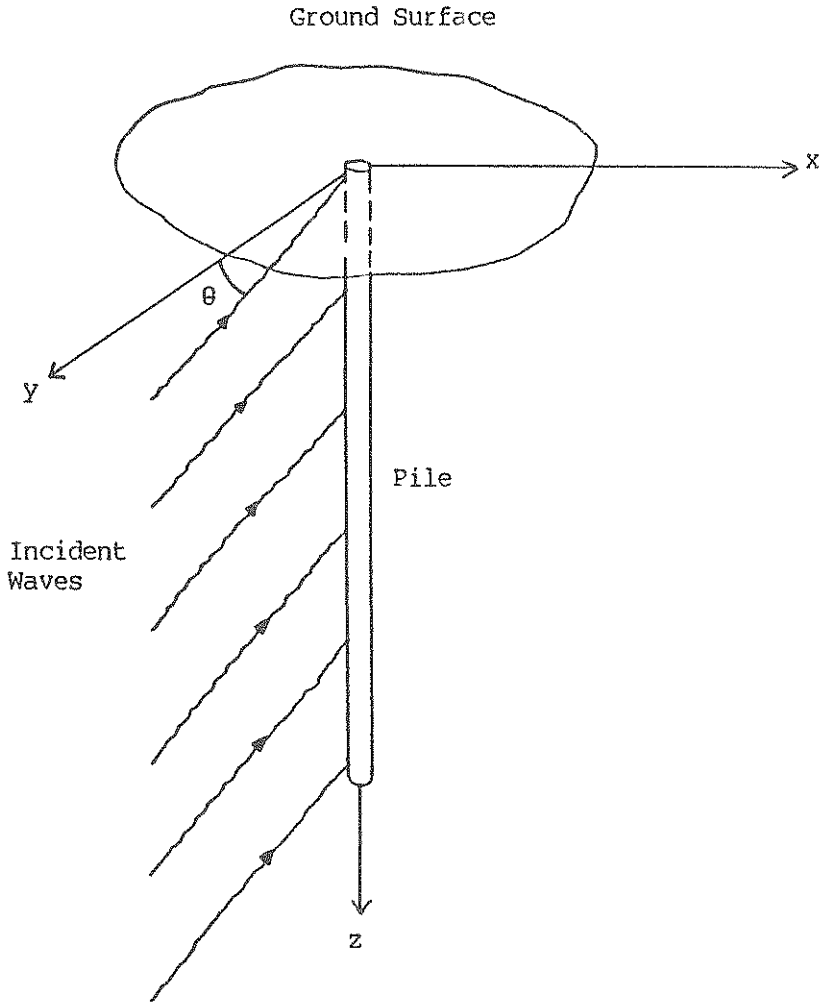

FIGURE 2-1. Model for Pile and System of Coordinates

where

$$f(x,t) = \exp(-\frac{i\omega lx}{C_s}) \cdot \exp(i\omega t) = \exp[i\omega(t - \frac{lx}{C_s})] \tag{2.23}$$

The shear stresses are obtained from the displacements by differentiation,

$$\tau_{xz} = -G(\frac{\omega n}{C_s}) \sin(\frac{\omega}{C_s} nz) \cdot f(x,t) \tag{2.24}$$

where G is the shear modulus.

Equations (2.22) and (2.24) directly furnish $\{u_s^f\}$ and $\{\phi_s^f\}$ variations along the depth in eq. (2.11) for SH-waves.

SV and P-Waves: In the case of SV and P-waves the horizontal displacement u_x and the vertical displacement u_z depend on both waves, but the formulation can be simplified assuming the same variation in the x-direction of all the displacement components. Equations similar to (2.22) and (2.24) can be written for axial and transverse stress and displacement values for this case, details of which are given in Ref. [9].

2.4 TRANSIENT ANALYSIS

The transient analysis has been done in the Laplace transform domain followed by a numerical inverse transformation to obtain the responses in the real time domain, a procedure which was previously used by Doyle [10], Cruse and Rizzo [8], Ahmad and Manolis [1], and others.

For transient analysis, the actual input is given as

$$u_x = \cos(\frac{\omega}{C_s} nz) \sin(\omega t - \frac{\omega lx}{C_s}) \tag{2.25}$$

$$\tau_{xz} = -G(\frac{\omega}{C_s} n) \sin(\frac{\omega}{C_s} n) \sin(\omega t - \frac{\omega lx}{C_s}) \tag{2.26}$$

For transient disturbances use is made of the Laplace transform of the field eqs. (2.25) and (2.26) with respect to time of the form [1,8]

$$f(x,s) = L\{f(x,t)\} = \int_0^\infty f(x,t)e^{-st}dt \qquad (2.27)$$

where 's' is the Laplace transformed parameter. The transformed domain integral equation representation does not require time convolutions that are necessary in a time domain formulation. Instead, the formulation is parametric in the transformed variable and the resulting algorithm involves the solution of a number of 'quasi-static' type equations.

Any internal viscous dissipation of energy can easily be accounted for by replacing the Lame constants λ and μ by their complex counterparts and leaving Poissons's ratio unaltered. The system matrices [G] and [D] in eq. (2.19) are dependent on the transform parameter s, and are thus complex. Equation (2.19) is solved for unknowns $\{u_p^t\}$ in terms of the prescribed boundary quantities $\{d_s\}$ and for a spectrum of values of the transform parameter. What remains to be done is to invert the solution back to the real time domain. The inverse Laplace transformation is defined as [1,8]:

$$f(x,t) = \frac{1}{2\pi i}\int_{\beta-i\infty}^{\beta+i\infty} f(x,s)\, e^{st}dS, \qquad i = \sqrt{-1} \qquad (2.28)$$

where $\beta > 0$ is arbitrary, but greater than the real part of all the singularities of f(s), and s is a complex number with $Re(s) > 0$. Details of the numerical inversion algorithm can be found in Ref. [1]. However, it has to be noted that the Laplace transform solution is essentially a superposition of a series of steady-state solutions and is therefore applicable only to linear problems. Also, since the Laplace transform casts the entire problem in the complex domain, the storage and computer time requirements are considerably increased.

SECTION 3

FUNDAMENTAL SOLUTION

3.1 INTRODUCTION

Implementation of the algorithm is dependent on the availability of the Green's function [3] for a dynamic point force buried in the interior of an elastic half-space. A boundary element formulation of the pile problem was recently reported by Kaynia and Kausel [13] who obtained (numerically) dynamic buried ring load (axial and lateral) solutions from the work of Apsel [2]. The major problem here is, of course, the accuracy of the numerically constructed dynamic solutions, since the convergence of the semi-infinite integrals in Apsel's work is heavily dependent on the frequency parameter.

An approximate solution [16] for the displacement field due to a point force e_j acting at a depth 'c' below the surface of the half-space can be constructed by superposing the displacement fields due to two dynamic forces acting within an infinite solid: one acts at a depth 'c' below the 'surface' and the other acts at a distance 'c' above the surface (i.e., the mirror image of the buried force); thus

$$u_i(x,\omega) = G^a_{ij}(x,\xi,\omega)e_j(\xi,\omega) \tag{3.1}$$

where

$$G^a_{ij} = G^o_{ij}(x,\xi',\omega) + G^o_{ij}(x,\xi'',\omega) \tag{3.2}$$

$$\xi' = (\xi_1,\xi_2,c) \quad \text{and} \quad \xi'' = (\xi_1,\xi_2,-c) \ .$$

The resulting stress field arising from G^a_{ij} does not completely satisfy the traction free-boundary conditions at the ground surface. In the aforementioned formulation, other fundamental solutions [15] such as double forces, line of forces, doublets, centers of compression, lines of

doublets, etc. are added on the negative side of the half-space to cancel the residual tractions. Therefore, the solution for the half-space can be expressed as

$$G_{ij}(x,\xi,\omega) = G^{a}_{ij}(x,\xi,\omega) + R_{ij}(x,\xi,\omega) \tag{3.3}$$

where the components of $R_{ij}(x,\xi,\omega)$ are contributed by the other fundamental solutions mentioned above.

This fundamental solution is derived by extending to the dynamic case of the superposition technique devised by Mindlin [18] for the half-space fundamental solution under static conditions. Mindlin's solution essentially consists of superposition of a combination of nuclei of strain [15] derived by synthesis from Kelvin's solution [14], such that the stresses vanish on the plane boundary of the half-space. Here the same procedure is employed by starting with the harmonic counterpart of Kelvin's solution in the Laplace's transformed domain [8]. In the following, only the various components of the residual functions are given. The problem is divided into two parts: (1) periodic force normal to the boundary; and (2) periodic force parallel to the boundary.

3.2 PERIODIC FORCE NORMAL TO THE BOUNDARY

The semi-infinite solid is considered to be bounded by the plane z=0, the positive z-axis penetrating into the body. A periodic dynamic force $pe^{i\omega t}$ is applied at point (0,0,+c) and acts in the positive z-direction (Fig. 3-1(a)), where ω is the circular frequency and i the imaginary unit. Since for this case, the displacement and stresses are symmetrical about the z-axis, the formulations have been derived in cylindrical coordinate systems. The solution for this case is compposed of six individual components, which in an unlimited solid, represent: (1) a single periodic dynamic force at (0,0,+c); (2) a single periodic dynamic force at (0,0,-c);

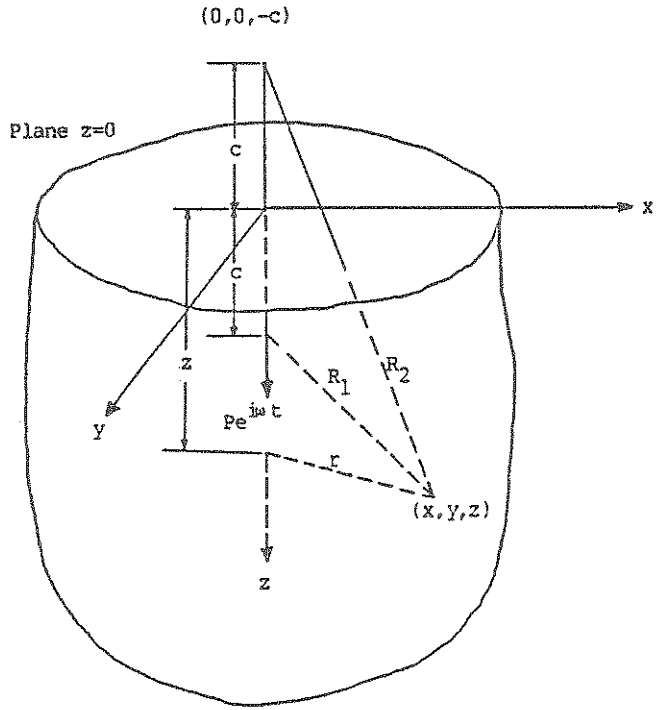

(a) Normal to the Boundary

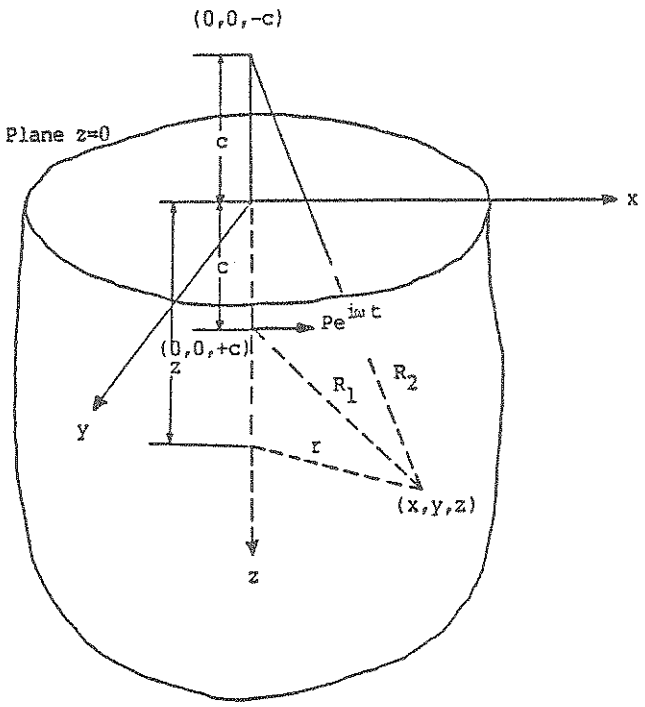

(b) Parallel to the Boundary

FIGURE 3-1. Periodic Force in the Interior of a Semi-infinite Solid

(3) a dynamic double force at (0,0,-c); (4) a dynamic center of compression at (0,0,-c); (5) a line of dynamic centers of compression extending from z = -c to z = -∞ and (6) a dynamic doublet at (0,0,-c).

1. Single periodic force at (0,0,+c)

The displacements in the r and z directions due to this are [8]:

$$U^1_{rz} = K_1 \left[- B_1 \left(\frac{\partial R_1}{\partial r}\right) \left(\frac{\partial R_1}{\partial z}\right)\right] \tag{3.4a}$$

$$U^1_{zz} = K_1 \left[A_1 - B_1 \left(\frac{\partial R_1}{\partial z}\right)^2\right] \tag{3.4b}$$

where R_1 is the distance between x and ξ. In addition,

$$K_1 = \frac{1}{4\pi\mu} \tag{3.4c}$$

$$A_1 = \left(\frac{c_2^2}{s^2R_1^2} + \frac{c_2}{sR_1} + 1\right) \frac{e^{-sR_1/c_2}}{R_1} - \frac{c_2^2}{c_1^2} \left(\frac{c_1^2}{s^2R_1^2} + \frac{c_1}{sR_1}\right) \frac{e^{-sR_1/c_1}}{R_1} \tag{3.4d}$$

$$B_1 = \left(\frac{3c_2^2}{s^2R_1^2} + \frac{3c_2}{sR_1} + 1\right) \frac{e^{-sR_1/c_2}}{R_1} - \frac{c_2^2}{c_1^2} \left(\frac{3c_1^2}{s^2R_1^2} + \frac{3c_1}{sR_1} + 1\right) \frac{e^{-sR_1/c_1}}{R_1} \tag{3.4e}$$

where

μ is the shear modulus,

c_1 and c_2 are the pressure and shear wave velocities, respectively, and

s is the Laplace transformed parameter which is equal to $-i\omega$ for the present case.

2. Single periodic force at (0,0,-c)

The expressions (U^2_{rz} and U^2_{zz}) due to this are exactly the same as (3.4a) to (3.4e) above, except that R_1 now has to be replaced by R_2, and

$$K_2 = \frac{3-4\nu}{4\pi\mu} \tag{3.5}$$

3. Dynamic double forces at (0,0,-c)

The displacement components are:

$$U^3_{rz} = K_3 \left[A_3\left(\frac{\partial R_2}{\partial z}\right)^2 - B_3\right] \left(\frac{\partial R_2}{\partial r}\right) \tag{3.6a}$$

$$U^3_{zz} = K_3 \left[A_3\left(\frac{\partial R_2}{\partial z}\right)^2 - C_3\right] \left(\frac{\partial R_2}{\partial z}\right) \tag{3.6b}$$

where

$$K_3 = -\frac{c}{2\pi\mu} \tag{3.6c}$$

$$A_3 = \left(\frac{15c_2^2}{s^2R_2^2} + \frac{15c_2}{sR_2} + \frac{sR_2}{c_2} + 6\right) \frac{e^{-sR_2/c_2}}{R_2^2}$$

$$- \frac{c_2^2}{c_1^2} \left(\frac{15c_1^2}{s^2R_2^2} + \frac{15c_1}{sR_2} + \frac{sR_2}{c_1} + 6\right) \frac{e^{-sR_2/c_1}}{R_2^2} \tag{3.6d}$$

$$B_3 = \left(\frac{3c_2^2}{s^2R_2^2} + \frac{3c_2}{sR_2} + 1\right) \frac{e^{-sR_2/c_2}}{R_2^2} - \frac{c_2^2}{c_1^2} \left(\frac{3c_1^2}{s^2R_2^2} + \frac{3c_1}{sR_2} + 1\right) \frac{e^{-sR_2/c_1}}{R_2^2} \tag{3.6e}$$

$$C_3 = \left(\frac{9c_2^2}{s^2R_2^2} + \frac{9c_2}{sR_2} + \frac{sR_2}{c_2} + 4\right) \frac{e^{-sR_2/c_2}}{R_2^2}$$

$$- \frac{3c_2^2}{c_1^2} \left(\frac{3c_1^2}{s^2R_2^2} + \frac{3c_1}{sR_2} + 1\right) \frac{e^{-sR_2/c_1}}{R_2^2} \tag{3.6f}$$

4. **Dynamic center of compression at (0,0,-c)**

The displacement components are

$$U^4_{rz} = K_4 \left[B_4 \left(\frac{\partial R_2}{\partial r}\right)\right] \tag{3.7a}$$

$$U^4_{zz} = K_4 \left[B_4 \left(\frac{\partial R_2}{\partial z}\right)\right] \tag{3.7b}$$

where

$$K_4 = \frac{c(1-2\nu)}{\pi\mu(3-4\nu)} \tag{3.7c}$$

$$B_4 = \left(\frac{3c_2^2}{s^2R_2^2} + \frac{3c_2}{sR_2} + 1\right) \frac{e^{-sR_2/c_2}}{R_2^2}$$

$$- \frac{c_2^2}{c_1^2} \left(\frac{3c_1^2}{s^2R_2^2} + \frac{3c_1}{sR_2} + \frac{sR_2}{c_1} + 2\right) \frac{e^{-sR_2/c_1}}{R_2^2} \tag{3.7d}$$

5. **Line of dynamic centers of compression extending from z = -c to z = -∞**

These are obtained by integrating expressions (3.7a) and (3.7b) above

$$U^5_{rz} = K_5 \int_{\xi=-c}^{-\infty} \left[B_5 \left(\frac{\partial R}{\partial r}\right)\right] d\xi \tag{3.8a}$$

$$U^5_{zz} = K_5 \int_{\xi=-c}^{-\infty} \left[B_5 \left(\frac{\partial R}{\partial z}\right)\right] d\xi \tag{3.8b}$$

where

$$K_5 = \frac{(1-\nu)(1-2\nu)}{\pi\mu(3-4\nu)} \tag{3.8c}$$

B_5 is the same as B_4 above, except that R_2 now has to be replaced by arbitrary $R = \{r^2+(z+\xi)^2\}^{1/2}$. This integral can be only evaluated numerically.

6. Dynamic doublet at (0,0,-c)

The displacement components are:

$$U^6_{rz} = K_6 \left[A_6 \left(\frac{\partial R_2}{\partial z}\right)\left(\frac{\partial R_2}{\partial r}\right)\right] \tag{3.9a}$$

$$U^6_{zz} = K_6 \left[A_6 \left(\frac{\partial R_2}{\partial z}\right) + B_6\right] \tag{3.9b}$$

where

$$K_6 = -\frac{c^2}{2\pi\mu(3-4\nu)} \tag{3.9c}$$

$$A_6 = -\left(\frac{15c_2^2}{s^2R_2^2} + \frac{15c_2}{sR_2} + \frac{sR_2}{c_2} + 6\right)\frac{e^{-sR_2/c_2}}{R_2^3}$$

$$+ \frac{c_2^2}{c_1^2}\left(\frac{15c_1^2}{s^2R_2^2} + \frac{15c_1}{sR_2} + \frac{s^2R_2^2}{c_1^2} + \frac{4sR_2}{c_1} + 9\right)\frac{e^{-sR_2/c_1}}{R_2^3} \tag{3.9d}$$

$$B_6 = \left(\frac{3c_2^2}{s^2R_2^2} + \frac{3c_2}{sR_2} + 1\right)\frac{e^{-sR_2/c_2}}{R_2^3} - \frac{c_2^2}{c_1^2}\left(\frac{3c_1^2}{s^2R_2^2} + \frac{3c_1}{sR_2} + \frac{sR_2}{c_1} + 2\right)\frac{e^{-sR_2/c_1}}{R_2^3} \tag{3.9e}$$

The addition of all the six components produce the complete solution U_{rz} and U_{zz}. When $s \rightarrow 0$, the expressions reduce identically to Mindlin's solution [18], of a (static) point force in the interior of a semi-infinite solid.

3.3 PERIODIC FORCE PARALLEL TO THE BOUNDARY

In this case there is no axial symmetry and it is therefore convenient to employ rectangular cartesian coordinates, (x,y,z). The periodic force

$Pe^{i\omega t}$ is applied at (0,0,+c) and acts in the positive x-direction (Fig. 3-1(b). For this case, the solution is composed of six individual components, which in an unlimited solid represent: (1) a single periodic dynamic force at (0,0,+c), (2) a single dynamic force at (0,0,-c), (3) a dynamic double force with moment at (0,0,-c), (4) a semi-infinite line of dynamic double forces with moment extending from z = -c to z = $-\infty$, (5) a dynamic doublet at (0,0,-c) and (6) a semi-infinite line of dynamic doublets extending from z = -c to z = $-\infty$ with strength proportional to the distance from z = -c.

1. Single periodic force at (0,0,+c)

The displacement components in x, y and z directions are [8]:

$$U^1_{xx} = L_1 \left[P_1 - Q_1 \left(\frac{\partial R_1}{\partial x}\right)^2\right] \tag{3.10a}$$

$$U^1_{yx} = L_1 \left[-Q_1 \left(\frac{\partial R_1}{\partial y}\right)\left(\frac{\partial R_1}{\partial x}\right)\right] \tag{3.10b}$$

$$U^1_{zx} = L_1 \left[-Q_1 \left(\frac{\partial R_1}{\partial z}\right)\left(\frac{\partial R_1}{\partial x}\right)\right] \tag{3.10c}$$

L_1, P_1 and Q_1 are the same as K_1, A_1 and B_1 in (3.4c), (3.4d) and (3.4e), respectively.

2. Single periodic force at (0,0,-c)

The expressions (U^2_{xx}, U^2_{yx} and U^2_{zx}) are the same as (3.10a) to (3.10c) above with R_1 replaced by R_2, and

$$L_2 = \frac{1}{4\pi\mu} \tag{3.11}$$

3. Dynamic double force with moment at (0,0,-c)

The displacement components are:

$$U^3_{xx} = L_3 \left[P_3\left(\frac{\partial R_2}{\partial x}\right)^2 - Q_3\right]\left(\frac{\partial R_2}{\partial z}\right) \tag{3.12a}$$

$$U^3_{yx} = L_3 \left[Q_3\left(\frac{\partial R_2}{\partial x}\right)\left(\frac{\partial R_2}{\partial y}\right)\left(\frac{\partial R_2}{\partial z}\right)\right] \tag{3.12b}$$

$$U^3_{zx} = L_3 \left[P_3\left(\frac{\partial R_2}{\partial z}\right)^2 - T_3\right]\left(\frac{\partial R_2}{\partial x}\right) \tag{3.12c}$$

where

$$L_3 = \frac{c}{2\pi\mu} \tag{3.12d}$$

$$P_3 = A_3 \tag{3.12e}$$

$$Q_3 = B_3 \tag{3.12f}$$

$$T_3 = \left(\frac{3c_2^2}{s^2R_2^2} + \frac{3c_2}{sR_2} + \frac{sR_2}{c_2} + 2\right)\frac{e^{-sR_2/c_2}}{R_2^2} - \frac{c_2^2}{c_1^2}\left(\frac{3c_1^2}{s^2R_2^2} + \frac{3c_1}{sR_2} + 1\right)\frac{e^{-sR_2/c_1}}{R_2^2} \tag{3.12g}$$

4. **Line of dynamic double forces with moment extending from z = -c to z = $-\infty$**

These are obtained by integrating expressions (3.12a), (3.12b) and (3.12c) above

$$U^4_{xx} = L_4 \int_{\xi=-c}^{-\infty} \left[P_4\left(\frac{\partial R}{\partial x}\right)^2 - Q_4\right]\left(\frac{\partial R}{\partial z}\right)d\xi \tag{3.13a}$$

$$U^4_{yx} = L_4 \int_{\xi=-c}^{-\infty} \left[P_4\left(\frac{\partial R}{\partial x}\right)\left(\frac{\partial R}{\partial y}\right)\left(\frac{\partial R}{\partial z}\right)\right]d\xi \tag{3.13b}$$

$$U^4_{zx} = L_4 \int_{\xi=-c}^{-\infty} \left[P_4\left(\frac{\partial R}{\partial z}\right)^2 - T_4\right]\left(\frac{\partial R}{\partial x}\right)d\xi \tag{3.13c}$$

where,

$$L_4 = -\frac{(1-2\nu)}{2\pi\mu} \tag{3.13d}$$

P_4, Q_4 and T_4 are the same as P_3, Q_3 and T_3 above, with R_2 replaced by arbitrary $R = \{x^2+y^2+(z+\xi)^2\}^{1/2}$.

5. **Dynamic doublets at (0,0,-c)**

The displacement components are:

$$U^5_{xx} = L_5 \left[P_5+Q_5\left(\frac{\partial R_2}{\partial x}\right)^2\right] \tag{3.14a}$$

$$U^5_{yx} = L_5\left[Q_5\left(\frac{\partial R_2}{\partial x}\right)\left(\frac{\partial R_2}{\partial y}\right)\right] \tag{3.14b}$$

$$U^5_{zx} = L_5\left[Q_5\left(\frac{\partial R_2}{\partial x}\right)\left(\frac{\partial R_2}{\partial z}\right)\right] \tag{3.14c}$$

where,

$$L_5 = K_6 \tag{3.14d}$$

$$P_5 = B_6 \tag{3.14e}$$

$$Q_5 = A_6 \tag{3.14f}$$

6. **Line of dynamic doublets extending from z = -c to z = -∞ with strength proportional to the distance from z = -c**

The displacement components are:

$$U^6_{xx} = L_6 \int_{\xi=-c}^{-\infty} \left[P_6+Q_6\left(\frac{\partial R}{\partial x}\right)^2\right](\xi-c)d\xi \tag{3.15a}$$

$$U^6_{yx} = L_6 \int_{\xi=-c}^{-\infty} \left[Q_6\left(\frac{\partial R}{\partial x}\right)\left(\frac{\partial R}{\partial y}\right)\right](\xi-c)d\xi \tag{3.15b}$$

$$U^{6}_{zx} = L_6 \int_{\xi=-c}^{-\infty} [Q_6(\frac{\partial R}{\partial x})(\frac{\partial R}{\partial z})](\xi-c)d\xi \qquad (3.15c)$$

where,

$$L_6 = -\frac{(1-\nu)(1-2\nu)}{\pi\mu(3-4\nu)} \qquad (3.15d)$$

P_6 and Q_6 are the same as P_5 and Q_5 respectively with R_2 replaced by arbitrary $R = \{x^2+y^2+(z+\xi)^2\}^{1/2}$.

The summation of all the six components furnish the complete solution U_{xx}, U_{yx} and U_{zx}. The limits $\rightarrow 0$, reduces to Mindlin's static solution [18]. Components U_{xy}, U_{yy} and U_{zy} can be similarly obtained.

SECTION 4

PRESENTATION AND ANALYSIS OF RESULTS

4.1 FORM OF PRESENTATION

This report presents the results of an extensive study on the seismic behavior of single piles in a non-dimensionless form. Among the groups of problem parameters influencing the response, most important are: the stiffness ratio E_p/E_s of the pile Young's modulus over a characteristic Young's modulus of the soil deposit; the slenderness ratio L/d of the length over the diameter of the pile frequency, and angle of incidence of the seismic waves. The dimensionless frequency parameter is defined as:

$$a_o = \frac{\omega d}{C_s} \tag{4.1}$$

where

ω circular frequency of excitation

d pile diameter

C_s shear wave velocity

The Young's modulus of soil is assumed to be constant with depth - typical of stiff overconsolidated clay deposits. The Poisson's ratio of the soil deposit was assumed to be 0.4. The ratio of the density of pile material to soil was taken as 1.6, typical of concrete piles. Material damping (β) was set equal to 0.05.

4.2 RESPONSES DUE TO SH-WAVES

The motion of the pile under the effects of SH-waves is considered first. Waves were assumed to produce a unit displacement on the free-field. The pile was modeled with eleven cylindrical elements. The displacement and tractions were assumed to be constant throughout each element.

The influence of E_p/E_s ratio is portrayed in Figs. 4-1(a) and 4-1(b) for a pile having L/d = 10 and 30 respectively and for a particular frequency (a_o = 0.5). The responses are shown for a vertically incident SH-wave (angle of incidence = 90^o). The figures show the variation along the depth of the ratio of the total transverse displacement, u_p^t to the free-field transverse displacement, u_f^g at the ground surface. It is seen that E_p/E_s ratio has a profound effect on the responses, at all depths. We observe high oscillatory variation for a very flexible pile (E_p/E_s = 100) and almost low, uniform rigid body motion for a very rigid pile. Also, for short piles (L/d = 10) bending moment is severe around the bottom mid-half of flexible piles - region particularly susceptible to fracture and/or yielding. A comparison between Figs. 4-1(a) and (b) reveals a profound difference between the behavior of short and long piles. Long piles are more susceptible to oscillatory responses even for stiffer piles.

Figures 4-2(a) and (b) show similar responses for a short and long pile respectively, but now for an obliquely incident wave (θ = 60) It is observed that for both the pile types the motions are higher as compared to a vertically incident wave. But still, the pile movements follow identical pattern.

Figures 4-3(a) and 4-3(b) show the ratio of the total horizontal pile motion, u_p^t to the free field motion, u_f^g at the top of a short pile (L/d = 10) to varying angles of incidence (θ = 45^o, 60^o, 75^o and 90^o), for a flexible and rigid pile, respectively. Figures 4-4(a) and 4-4(b) show the same variation for a long pile (L/d = 30). It can be seen that the angle of incidence and the stiffness ratio have a profound influence on the filtering effects. It is observed that in the low frequency range, the filtering effects increase with the angle of incidence, but this is not true for all frequencies due to oscillations of the results. Resonant

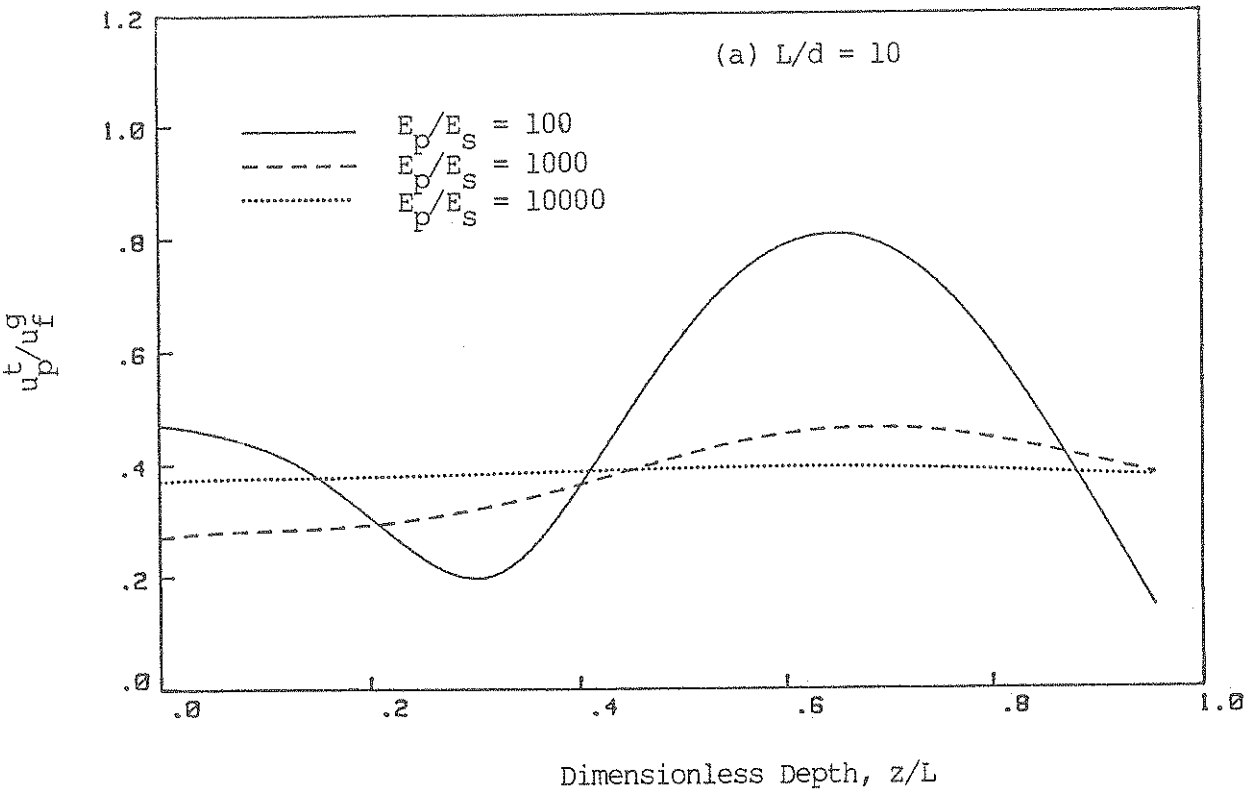

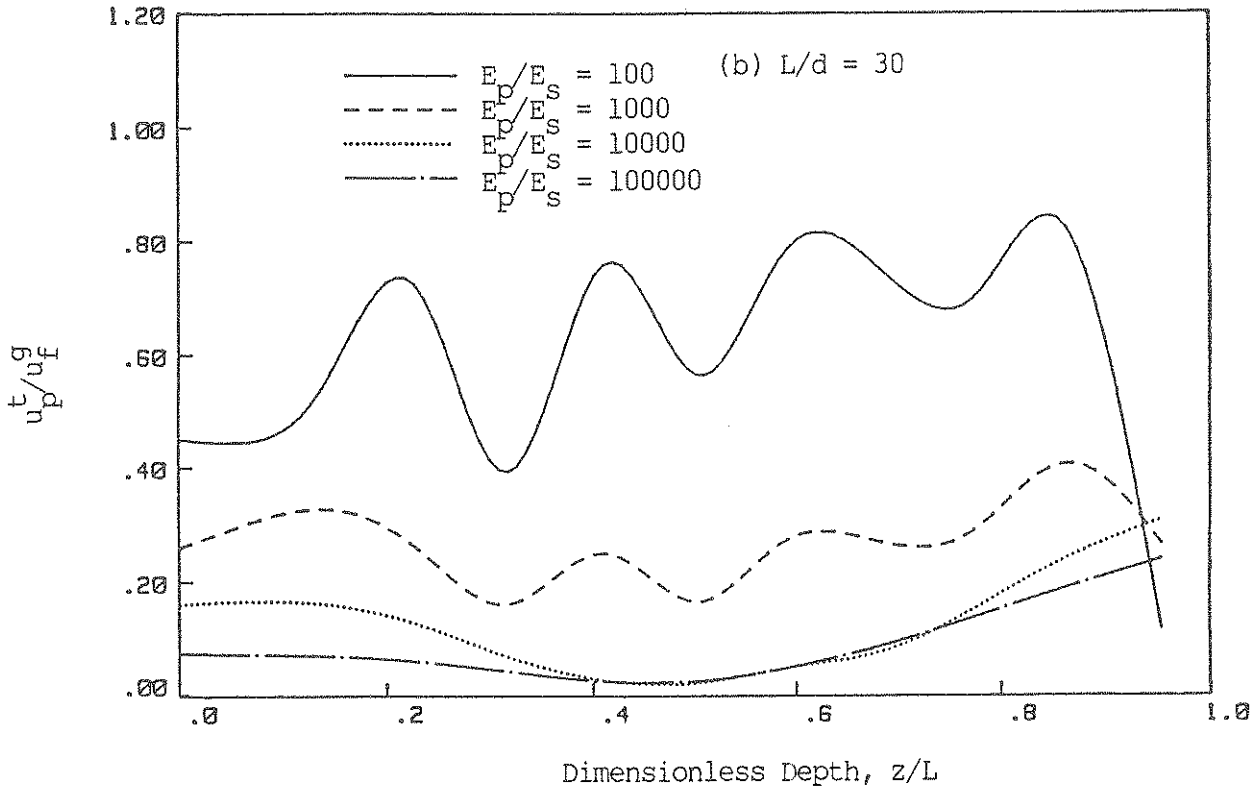

Figure 4-1. Transverse Displacement Ratios for Vertically Incident SH-Waves

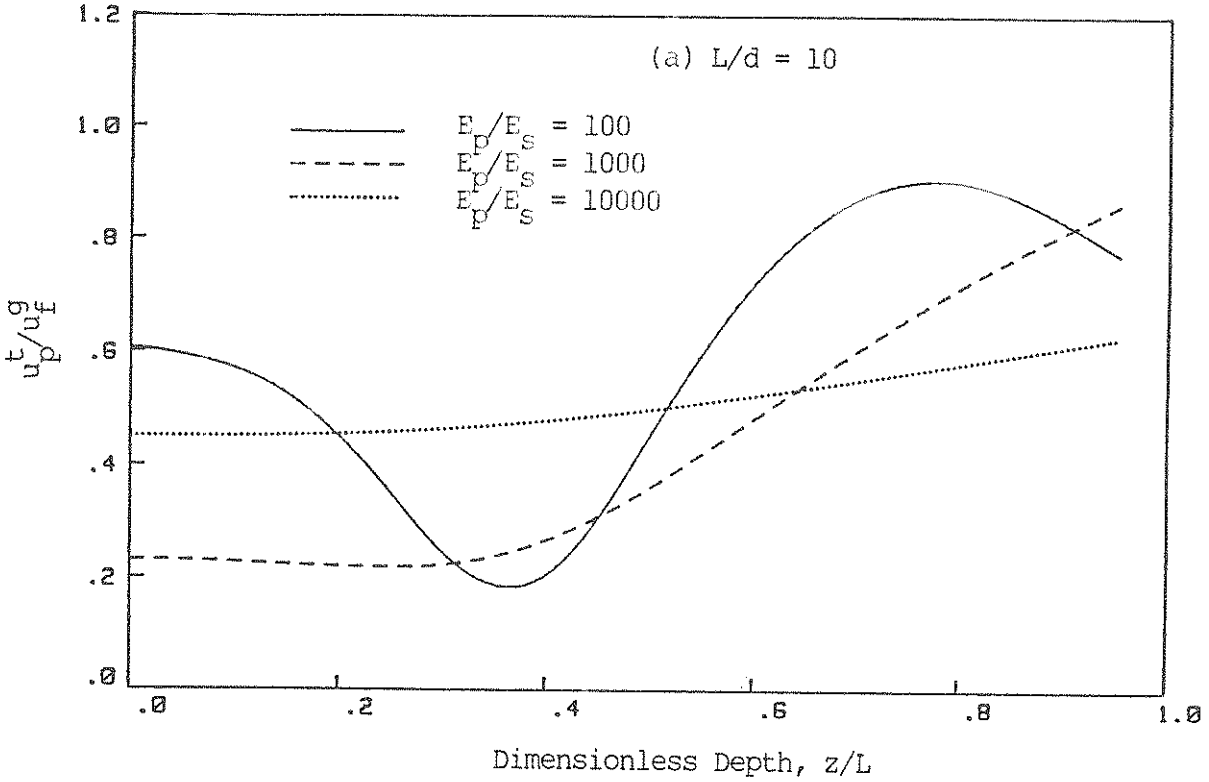

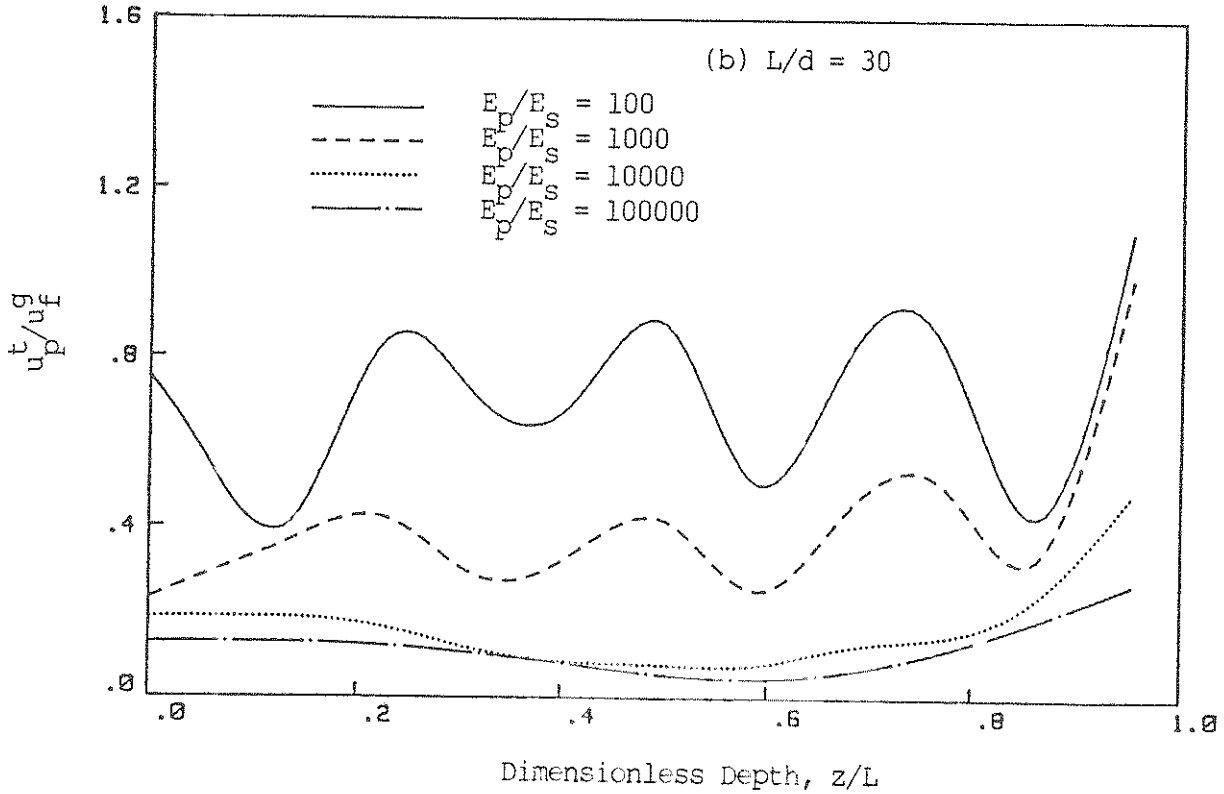

Figure 4-2. Transverse Displacement Ratios for Obliquely Incident SH-Waves ($\theta = 60^{o}$)

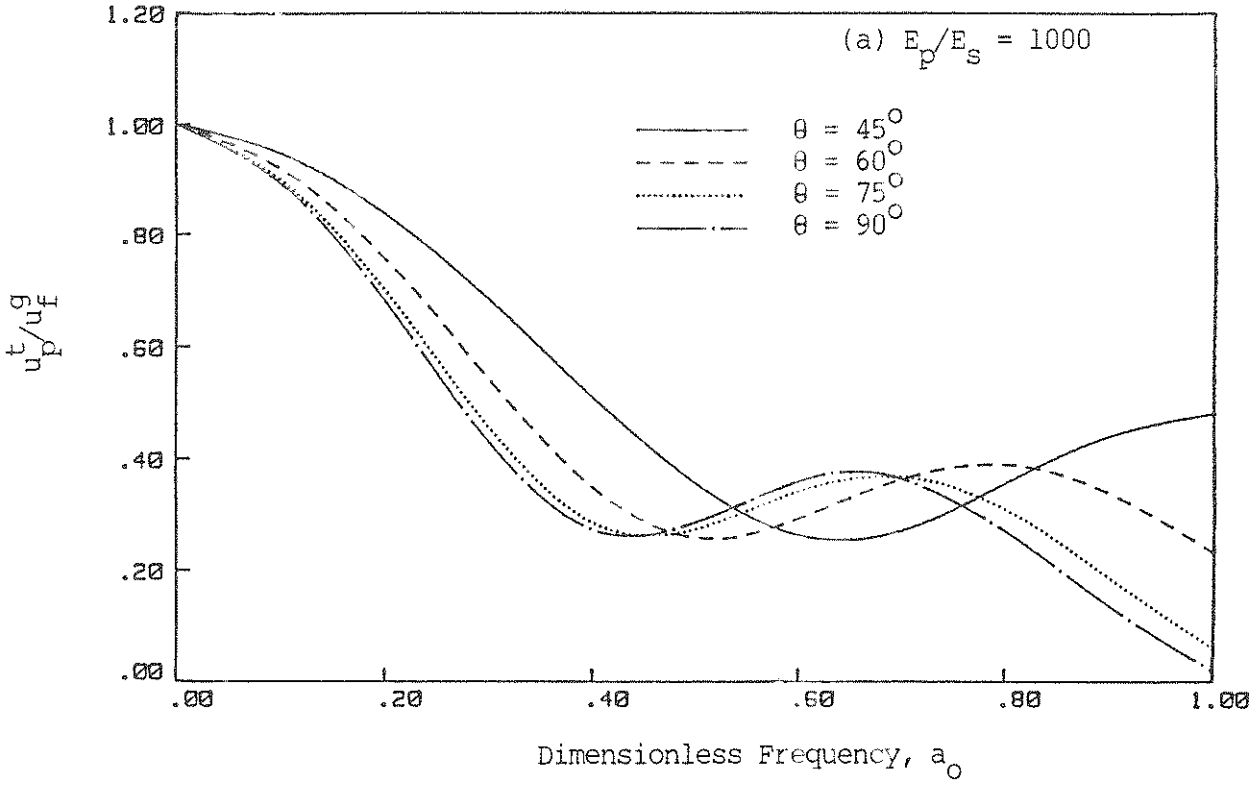

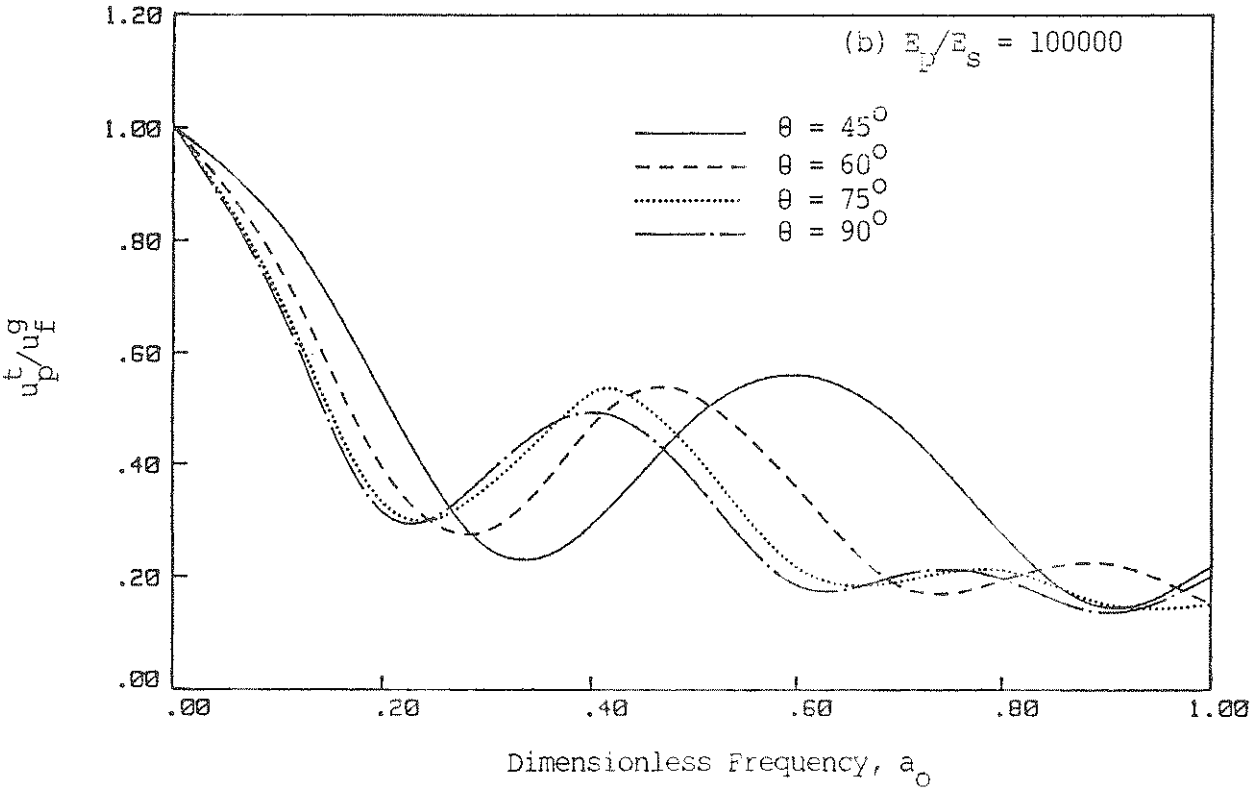

Figure 4-3. Transverse Displacement Ratios for SH-Waves in a Short Pile

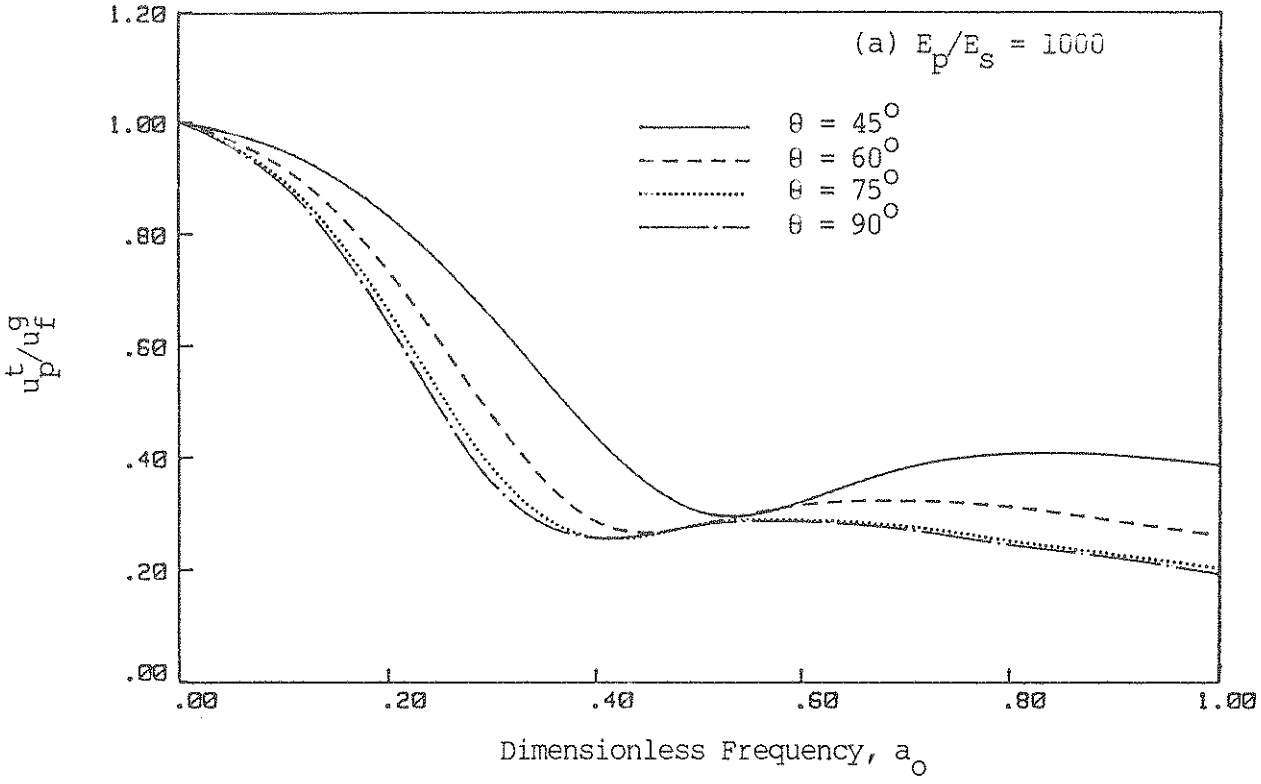

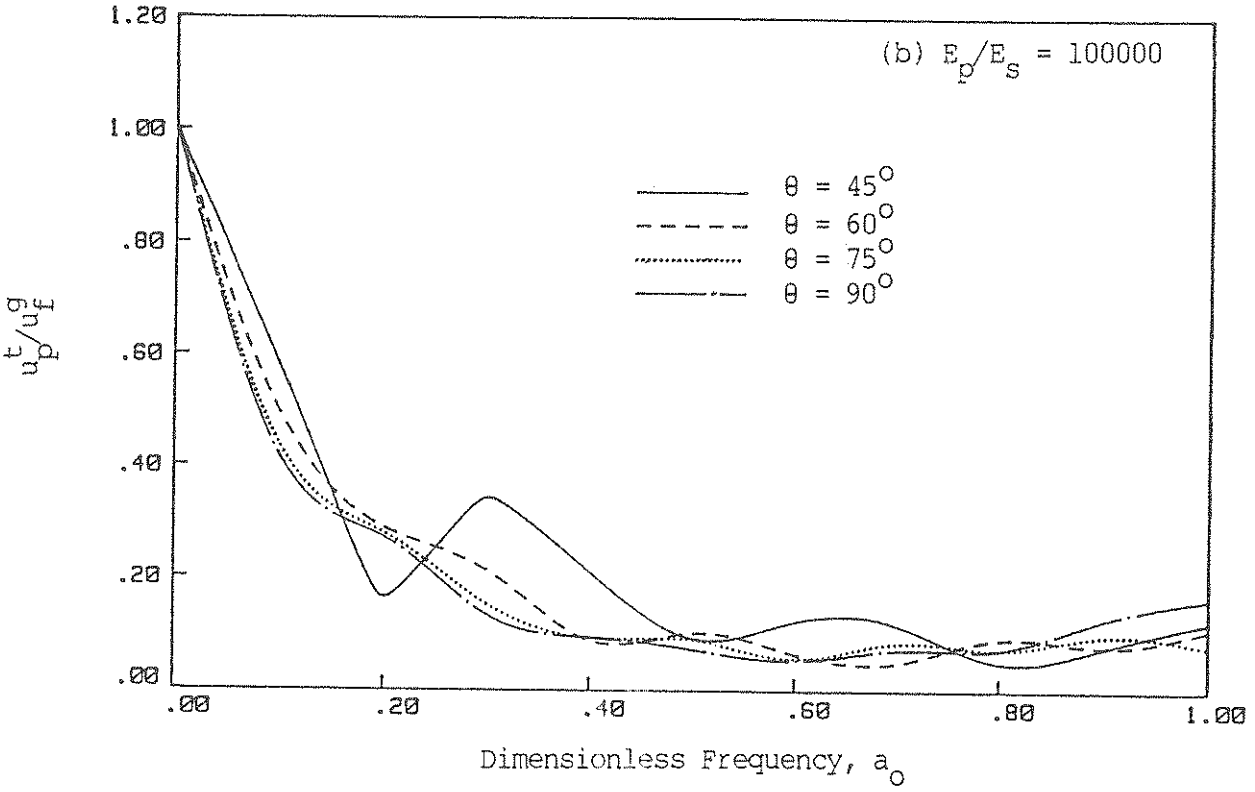

Figure 4-4. Transverse Displacement Ratios for SH-Waves in a Long Pile

peaks occur at a lower frequency for a vertically incident wave than obliquely incident ones. Filtering effects increase more rapidly for a very rigid pile than for a flexible one. This is particularly true for longer piles where the motions rapidly reduce to negligible values at higher frequencies.

4.3 RESPONSES DUE TO P AND SV-WAVES

The motion of single piles under the influence of a combination of P and SV-waves are considered next. As in the case of SH-waves the results will be presented as a function of the normalized depth, z/L and the dimensionless frequency parameter, a_o. Incident waves are assumed to produce a unit displacement on the free-field. For vertically incident waves the pile variations will be equal to that obtained when only an S-wave is considered (SV and SH-waves are the same for $\theta = 90^o$).

Figures 4-5(a) and 4-5(b) show the variation of axial displacement ratio, u_p^t versus the free field axial ground motion, u_f^g for an obliquely incident combination of P and SV-waves ($\theta = 75^o$) for a particular frequency ($a_o = 0.5$), for a short and long pile, respectively. Corresponding transverse displacement ratios are portrayed in Figs. 4-6(a) and 4-6(b). As in the case of SH-waves, the stiffness ratio and the embedment length have significant influence on the responses. Whereas, a rigid pile shows almost a uniform rigid body motion, flexible piles exhibit oscillatory movements, resulting in unacceptable amounts of moments that could cause yielding and/or fracture of the pile.

The transverse displacement ratios u_p^t/u_f^g at the top of the pile is depicted in Figs. 4-7(a) and 4-7(b) for a short and long pile respectively with E_p/E_s equal to 1000. Here again we observe the increase in the filtering effects with the angle of incidence. For a vertically incident wave ($\theta = 90^o$) the results are identical to those in Fig. 4-3(a) and 4-4(a)

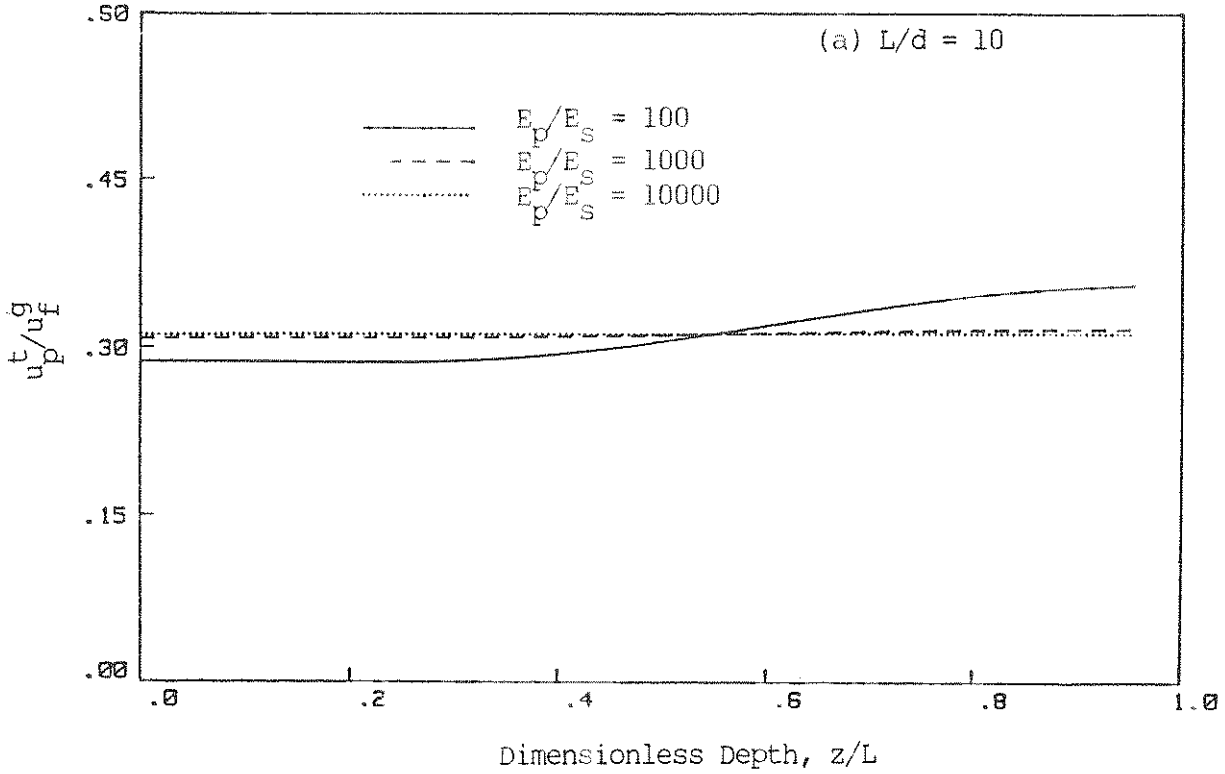

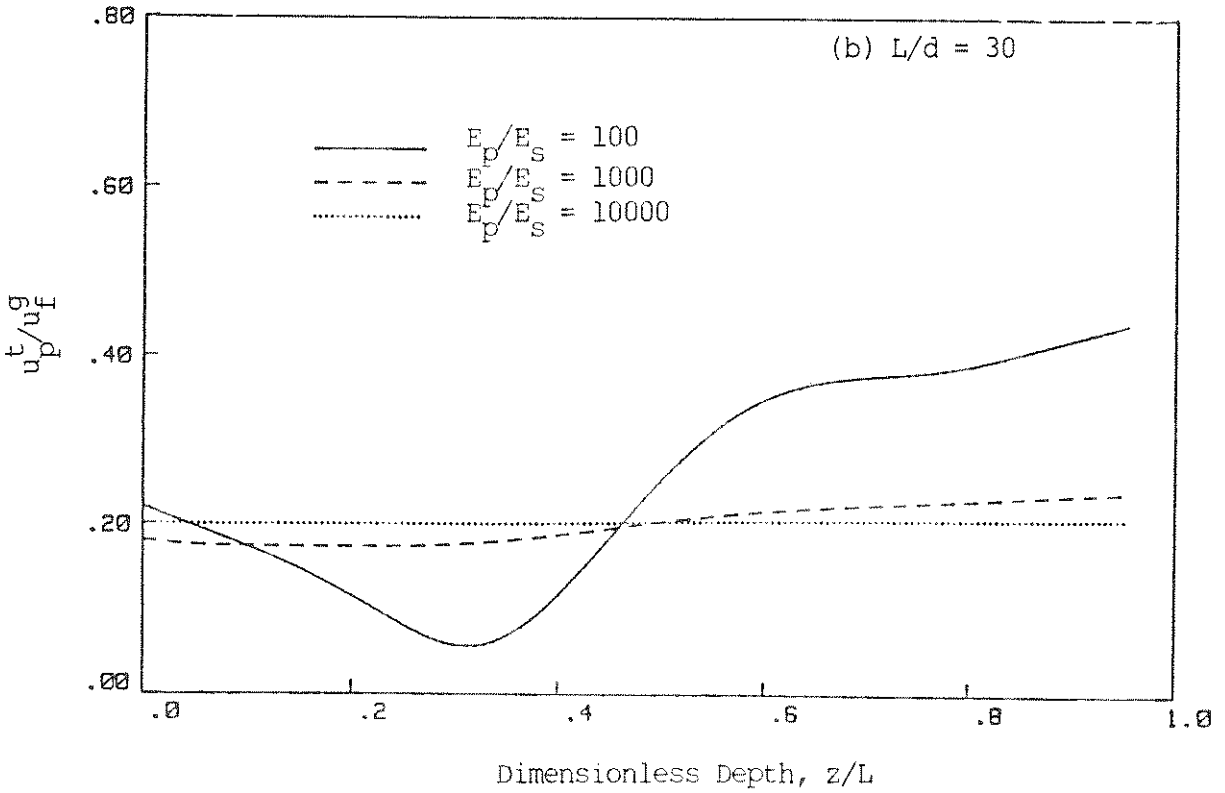

Figure 4-5. Axial Displacement Ratios for Obliquely Incident P and SV-Waves ($\theta = 75^{\circ}$)

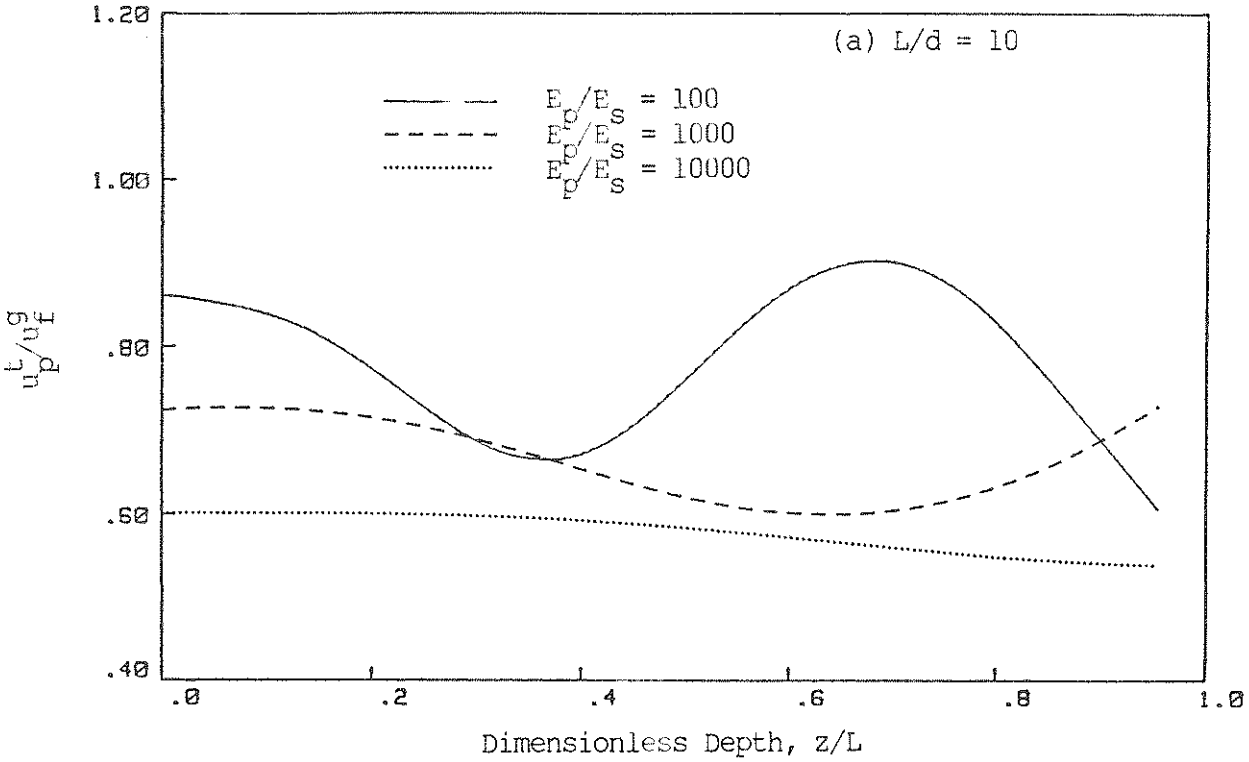

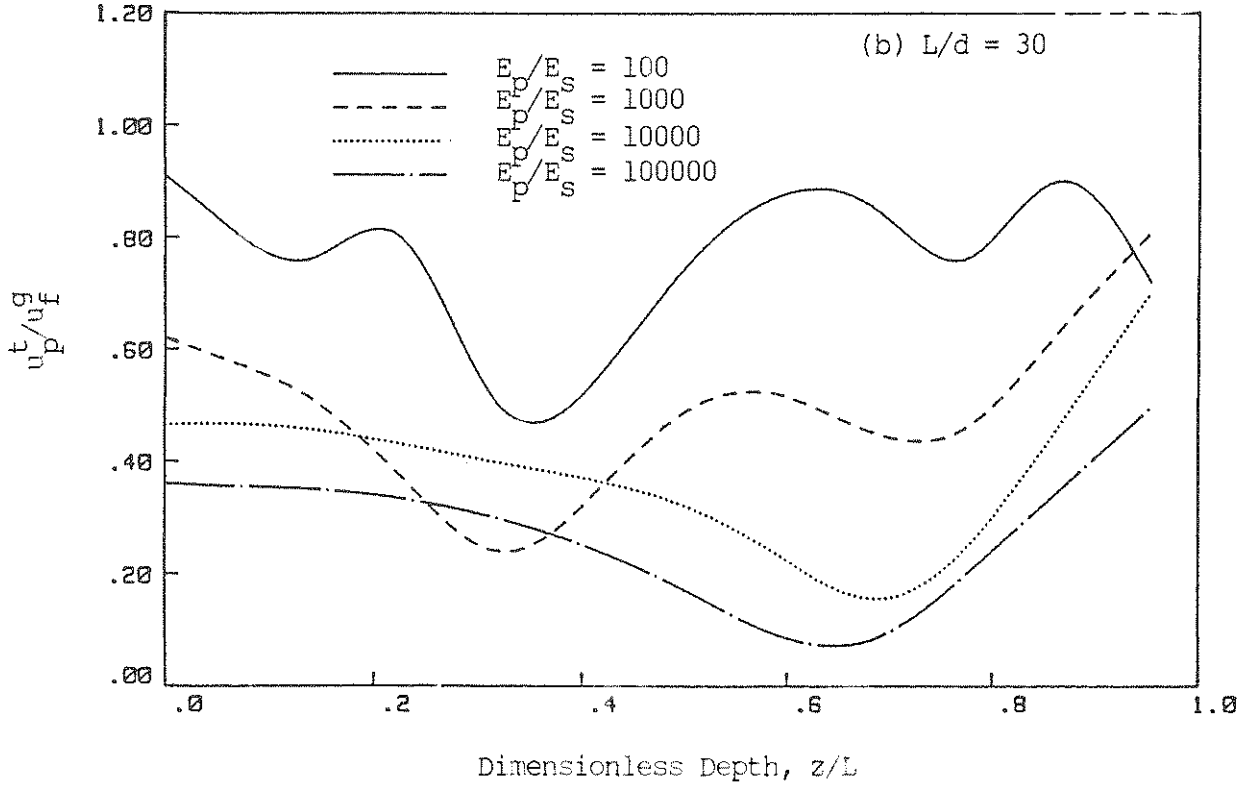

Figure 4-6. Transverse Displacement Ratios for Obliquely Incident P and SV-Waves ($\theta = 75^{\circ}$)

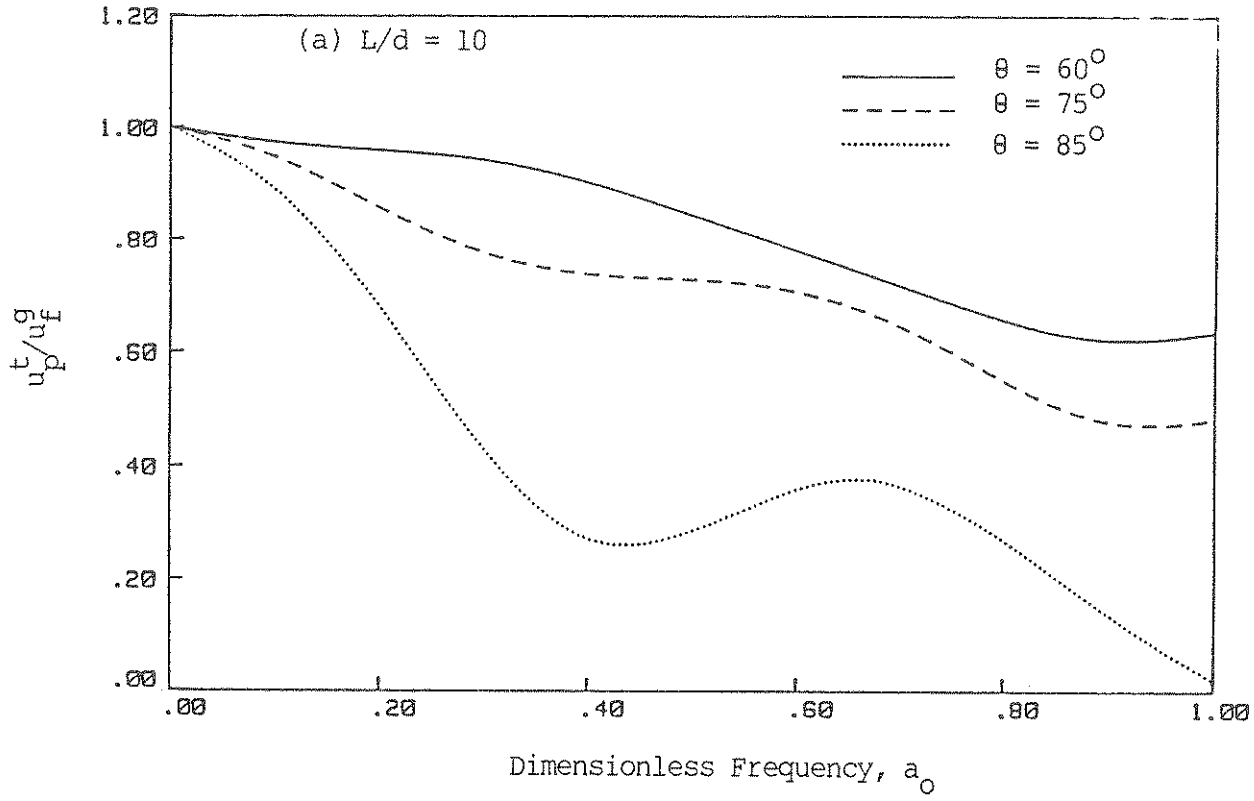

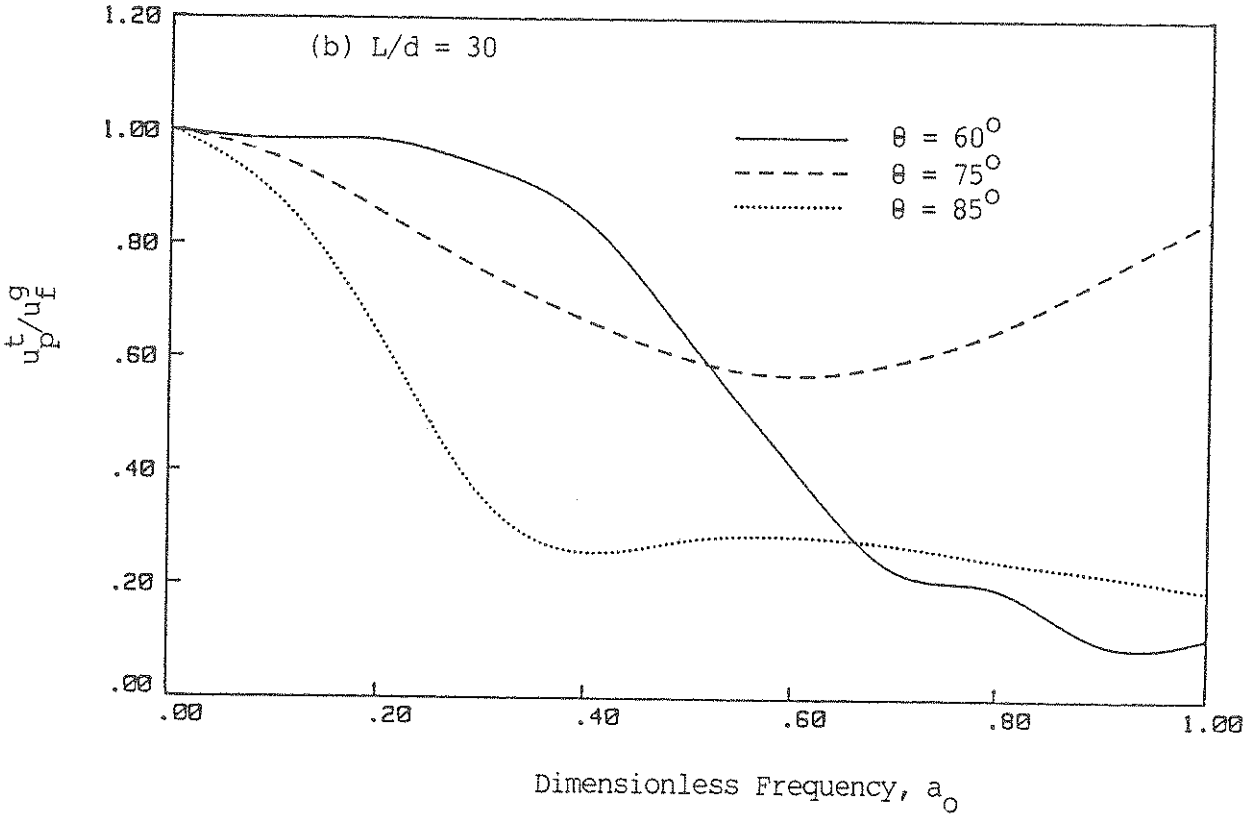

Figure 4-7. Transverse Displacement Ratios for P and SV-Waves (E_p/E_s = 1000)

when only an SH-wave was considered.

The practical significance of all such curves are apparent: by multiplying a given free-field design response spectrum with the appropriate interaction curve, one may obtain the design response spectrum that must be input at the base of a structure on pile foundations.

4.4 TRANSIENT RESULTS

For the transient analysis, equations (2.25) and (2.26) represent the input free-field excitation. The excitation frequency, ω is set equal to 0.5 rad/sec and the time axis is normalized with respect to the shear wave velocity (C_s) and a characteristic length of the pile as

$$\bar{t} = \frac{C_s t}{L} \tag{4.2}$$

Figures 4-8(a) and (b) show the actual transverse displacement, at the mid length of the pile, for a short and long pile respectively due to vertically incident wave. It is observed that, presence of the pile alters the free-field displacement values substantially. Whereas, rigid piles show small or negligible movement, flexible piles appear to follow the ground motions. This observation is more pronounced for longer piles.

Figures 4-9(a) and (b) show the corresponding values for an obliquely incident wave ($\theta = 60^{o}$). Here also rigid piles exhibit negligible displacement and flexible piles experience higher motion. This phenomena is more pronounced for longer piles, but still, the magnitudes are much lower than the corresponding values for a vertically incident wave.

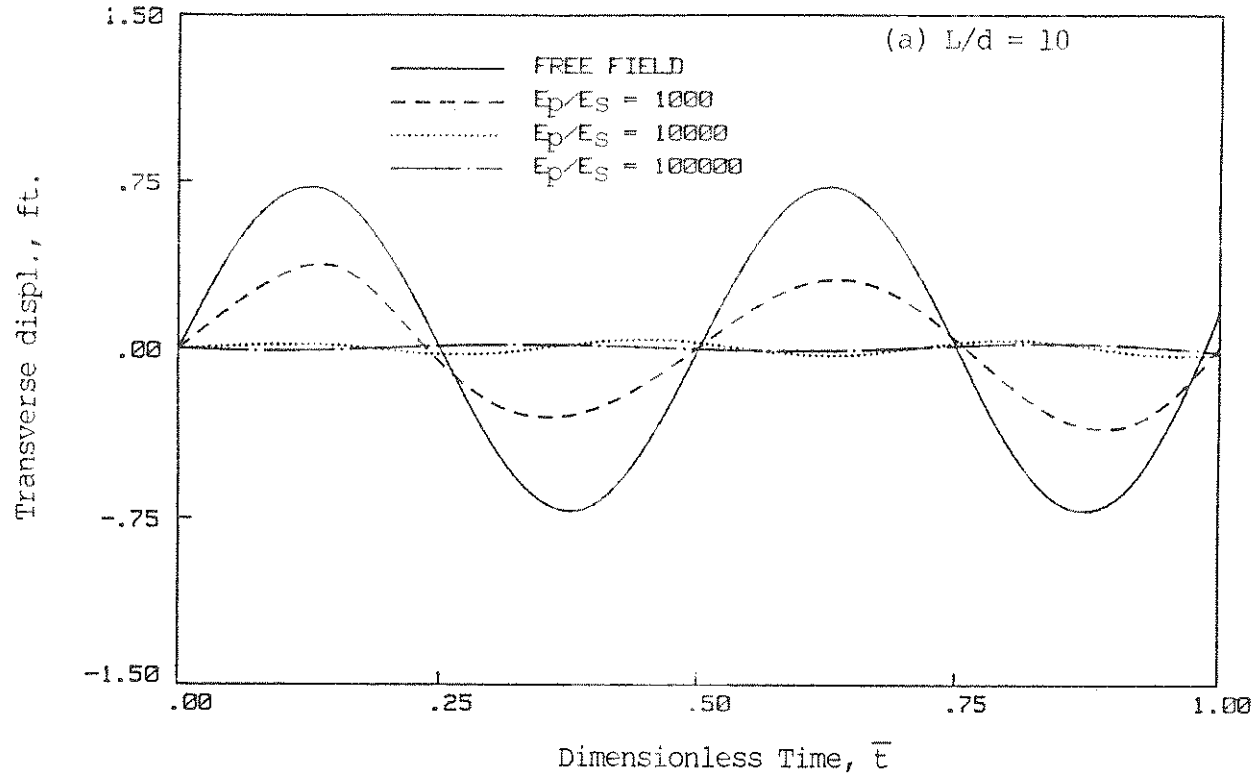

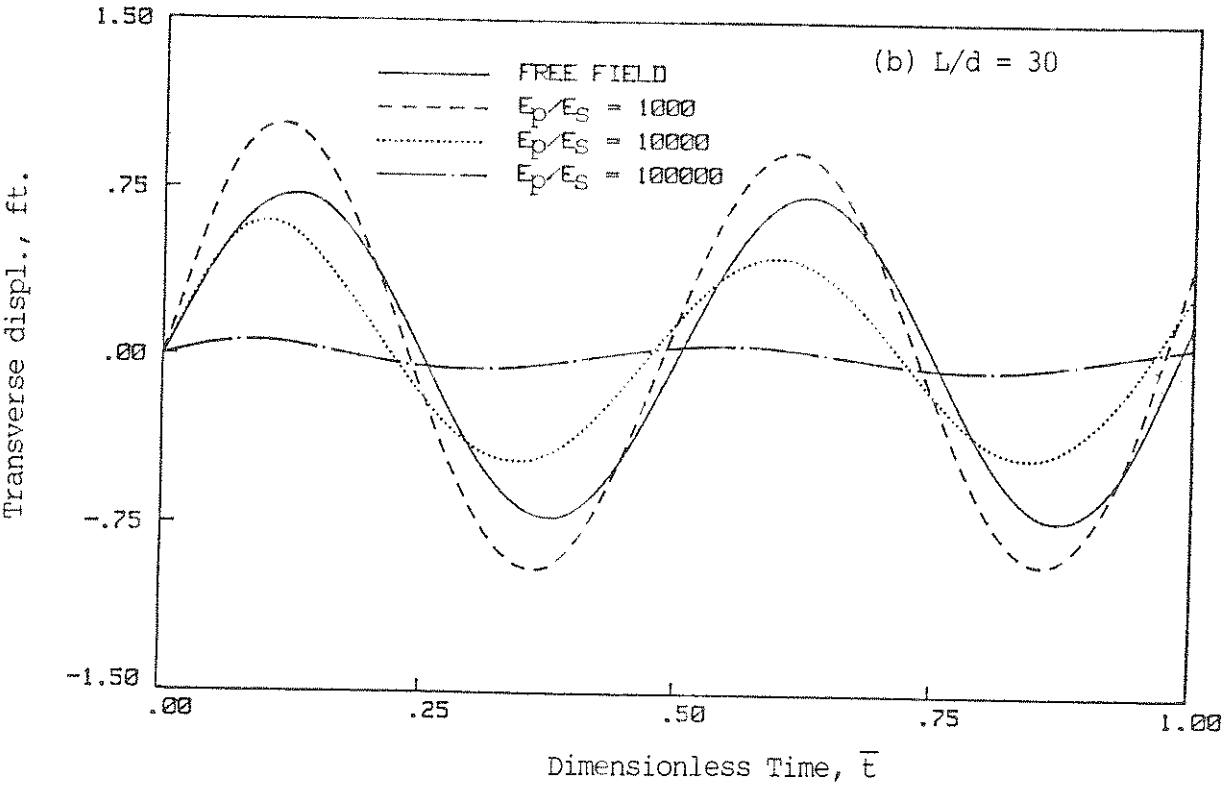

Figure 4-8. Transverse Displacements for Vertically Incident Waves ($\theta = 90^{o}$)

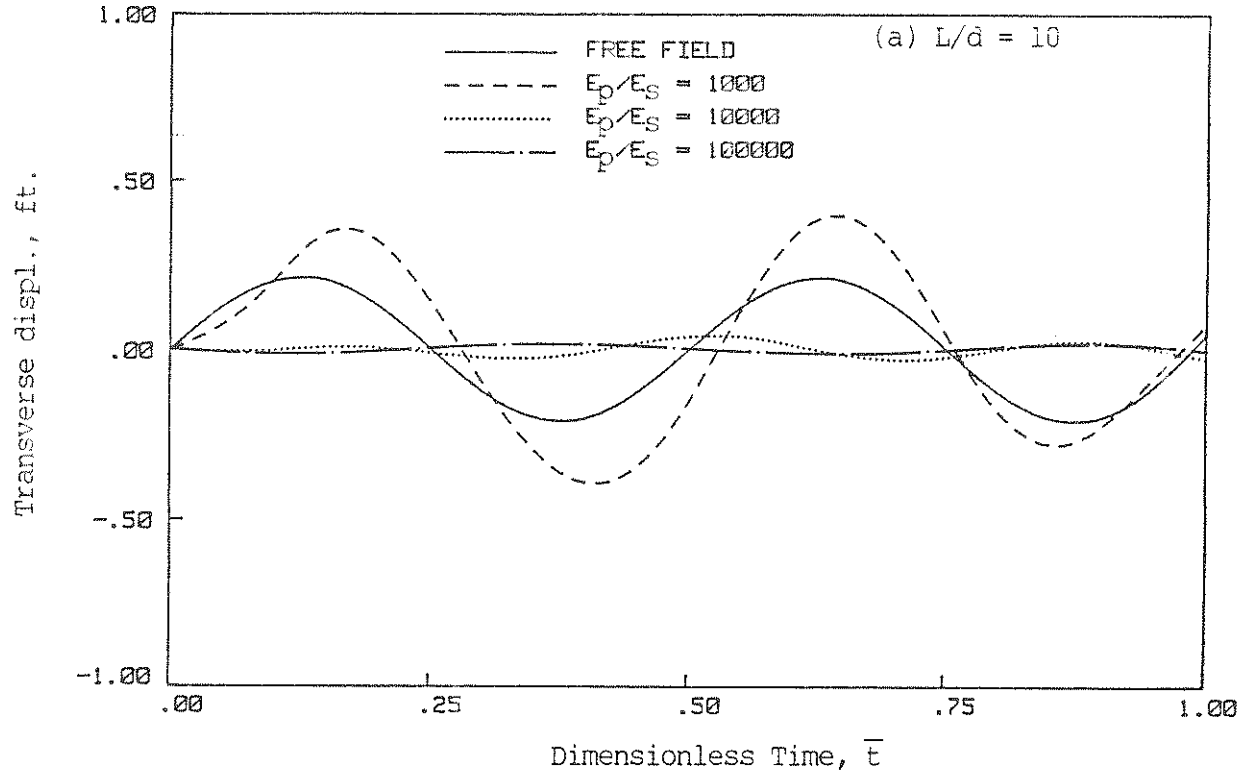

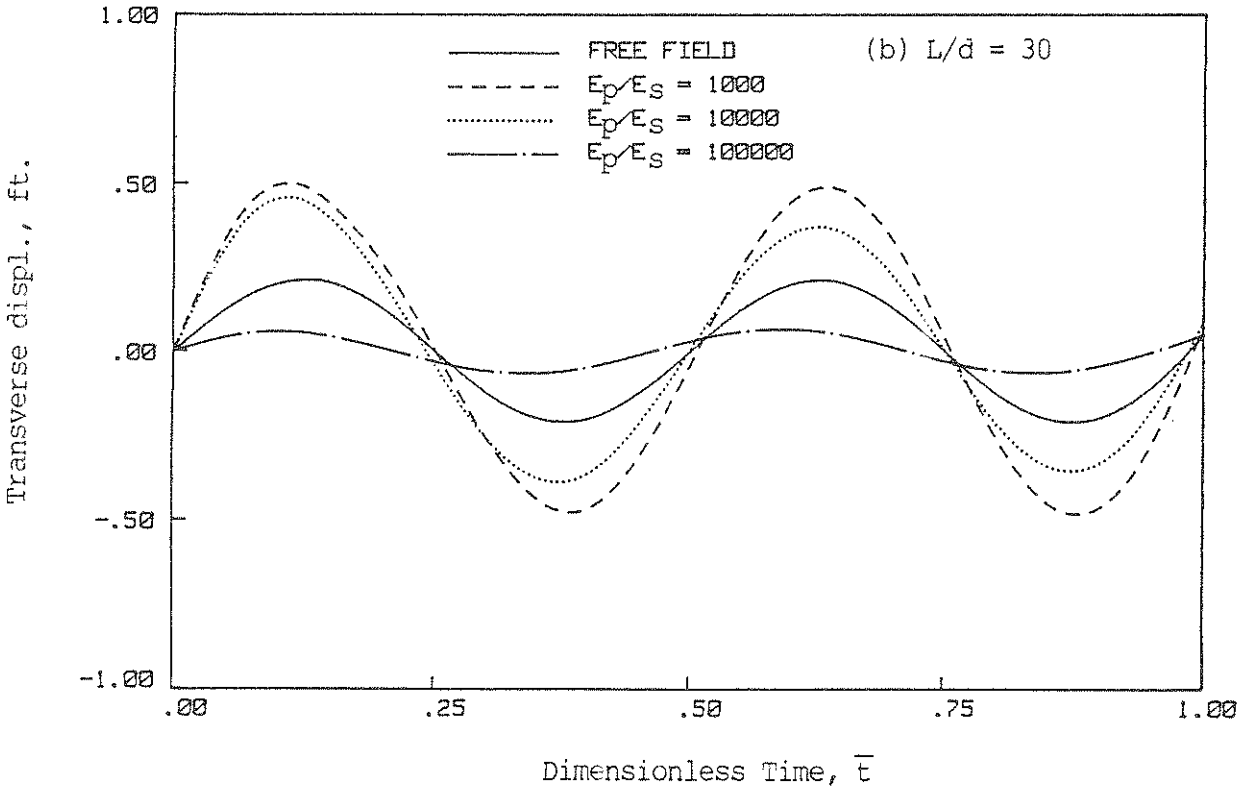

Figure 4-9. Transverse Displacements for Obliquely Incident Waves ($\theta = 60^{o}$)

SECTION 5

CONCLUSIONS

Responses of piles to vertically and obliquely incident SH, SV and P waves have been analyzed. It is found that the stiffness ratio, angle of incidence and the excitation frequency have a significant influence on the pile response. While the number of cases studied is not sufficiently large to derive approximate formulae or general conclusions, it appears that the existence of the pile foundation produces a filtering of the waves, reducing the amplitude of the motion as a function of frequency. Longer piles are more susceptible to oscillatory response even with higher stiffness.

For short flexible piles, bending moment is found to be severe around the bottom half of the pile. Filtering effects increase more rapidly for a rigid pile than for a flexible one. Resonant peaks occur at a lower frequency for a vertically incident wave than obliquely incident ones. Finally, the pilot transient analysis also indicates that the presence of the pile modifies the ground motion substantially.

The interaction curves presented in this report have significant practical utility. A design response spectrum for a structure resting on a pile foundation may be readily obtained by multiplying a given free-field design response spectrum with the appropriate interaction curve.

SECTION 6

NOTATION

a_o	dimensionless frequency parameter defined by equation (4.1)
A_1 to A_6	expressions defined in Section 3.1
A_b	cross sectional area of pile base
A_p	cross sectional area of pile
A_{SH}	amplitudes of incident SH waves
A'_{SH}	amplitudes of reflected SH waves
[B]	matrix defined in equation (2.15)
B_1 to B_6	expressions defined in Section 3.1
$\{b_p\}$	displacement vector for unit pile head b.c.
$\{b_s\}$	known vector defined by equation (2.11)
c	depth of source from free surface of half space
C_p, c_1	pressure wave velocity
C_s, c_2	shear wave velocity
d	pile diameter
$\{d_s\}$	matrix defined in equation (2.18)
[D]	pile compressibility and flexibility matrix
[E]	matrix defined in equation (2.17)

E_p	Young's modulus of pile material
E_s	Young's modulus of soil material
η	parameter defined by equation (2.13b)
$\{\phi_i\}$	vector of pile-soil interface tractions
$\{\phi_b\}$	axial pile stress at base
$\{\phi_x\}$	vector of lateral pile traction
$\{\phi_z\}$	vector of axial pile traction
$\{\phi_p^t\}$	vector of total field pile tractions
$\{\phi_s^f\}$	vector of free field soil tractions
$\{\phi_s^s\}$	vector of scattered field soil tractions
$\{\phi_s^t\}$	vector of total field soil tractions
$[G_{ij}]$	Green's function
γ	parameter defined by equation (2.13a)
i	imaginary unit, $\sqrt{-1}$
I_p	moment of inertia of pile cross section
K_1 to K_6	constants defined in Section 3.1
l	direction cosine of propagation of SH wave
L	length of pile
L_1 to L_6	constants defined in Section 3.2

λ	Lame's constant
m	mass per unit length of pile
M(z)	bending moment at depth z of pile
μ	Lame's constant
n	direction cosine of propagation of SH wave
	Poisson's ratio
P_1 to P_6	expressions defined in Section 3.2
$P_x(z)$	transverse load at depth z of pile
$P_z(z)$	axial load at depth of z of pile
π	3.141592654
Q_1 to Q_6	expressions defined in Section 3.2
r	component in polar axes system
R_1	distance between field point and real source point
R_2	distance between field point and image source point
$[R_{ij}]$	residual terms in Green's function
ρ	density of pile material
s	Laplace's transform parameter
t	time
$\bar{t}$	dimensionless time defined by equation (4.2)

θ inclination angle of seismic waves

u_1 pile head displacement

U_{ij} displacements in ith direction due to force in jth direction

U_i acceleration component in ith direction

$\{u_x\}$ lateral pile displacements

$\{u_z\}$ axial pile displacements

$\{u_p^t\}$ vector of total field pile displacements

$\{u_s^f\}$ vector of free field soil displacements

$\{u_s^s\}$ vector of scattered soil displacements

$\{u_s^t\}$ vector of total soil displacements

ω circular frequency

ξ integration parameter

SECTION 7

REFERENCES

1. Ahmad, S. and Manolis, G.D., 'Dynamic Analysis of 3-D Structures by a Transformed Boundary Element Method,' Computational Mechanics, Vol. 2, 1987, pp. 185-196.

2. Apsel, R., 'Dynamic Green's Functions for Layered Media and Applications to Boundary Value Problems,' Ph.D. Thesis, Dept. of Appl. Mech. and Eng. Sci., Univeristy of California, San Diego, 1979.

3. Banerjee, P.K. and Butterfield, R., Boundary Element Methods in Engineering Sciences, Mc-Graw Hill, London and New York, 1981.

4. Banerjee, P.K., 'Analysis of Axially and Laterally Loaded Pile Groups,' in C.R. Scott (ed.) Developments in Soil Mechanics, Applied Science Publishers, London, Chapter 9, 1978, pp. 317-346.

5. Banerjee, P.K. and Driscoll, R.M., 'Three-dimensional Analysis of Raked Pile Groups,' Proc. Instn. of Civil Engrs., Part 2, Vol. 61, 1976, pp. 653-671.

6. Banerjee, P.K. and Sen, R., Dynamic Behavior of Axially and Laterally Loaded Piles and Pile Groups, Chapter 3 in Dynamic Behavior of Foundations and Buried Structures (Developments in Soil Mech. Foundation Engineering, Vol. 3), Ed. P.K. Banerjee and R. Butterfield, Elsevier Applied Science, London, pp. 95-133, 1987.

7. Banerjee, P.K., Sen, R. and Davies, T.G., Static and Dynamic Analyses of Axially and Laterally Loaded Piles and Pile Groups, Chapter 7 in Geotechical Modeling and Applications (Dean Alexander Vesic Memorial Volume), Ed. S.M. Sayed, Gulf Publishing Co., Houston, pp. 322-354, 1987.

8. Cruse, T.A. and Rizzo, F.J., 'A Direct Formulation and Numerical Solution of the General Transient Elastodynamic Problem, I,' Journal of Anal. and Appl. Math., Vol. 22, 1968, pp. 244-259.

9. Dominguez, J and Roesset, J.M., 'Response of Embedded Foundations to Travelling Waves,' Report No. R78-24, Dept. of Civil Engr., MIT, Cambridge, MA, 1978.

10. Doyle,J.M., 'Integration of the Laplace Transformed Equations of Classical Kinetics,' Journal of Appl. Math., Vol. 13, 1966.

11. Flores-Berrones, R. and Whitman, R.V., 'Seismic Responses of End Bearing Piles,' Journal of Geotech. Eng., ASCE, Vol. 108, GT4, 1982, pp. 554-569.

12. Gazetas, G., 'Seismic Responses of End Bearing Single Piles,' Soil Dynamics and Earthq. Eng., Vol. 3, No. 2, 1984, pp. 82-93.

13. Kaynia, A.M. and Kausel, E., 'Dynamic Behavior of Pile Groups,' 2nd Int. Conf. on Num. Methods in Offshore Piling, Austin, TX, 1982.

14. Kelvin, (Lord), 'Displacements Due to a Point Load in an Indefinitely Extended Solid,' Math. and Phys. Papers, London, Vol. 1, 1848, pp. 97.

15. Love, A.E.H., A Treatise on the Mathematical Theory of Elasticity, 4th Ed., Cambridge University Press, London, 1952.

16. Mamoon, S.M., Ahmad, S., and Banerjee, P.K., 'Seismic Behavior of Pile Foundations,' Status Report, National Center for Earthquake Engineering Research, State University of New York at Buffalo, May 1988.

17. Michalopoulos, E., 'Amplification of Generalized Surface Waves,' M.S. Thesis, Department of Civil Engineering, MIT, Cambridge, MA, 1976.

18. Mindlin, R.D., 'Force at a Point in the Interior of a Semi-infinite Solid,' Journal of Applied Physics, Vol. 7, 1936, pp. 195-202.

19. Poulos, H.G. and Davis, E.H., Pile Foundation Analysis and Design, John Wiley and Sons, Inc., New York, New York, 1980.

20. Sen, R., Davies, T.G., and Banerjee, P.K., 'Dynamic Analysis of Axially and Laterally Loaded Piles and Pile Groups Embedded in Homogeneous Soils,' Journal of Earthq. Eng. and Struct. Dyn., Vol. 13, 1985, pp. 53-65.

21. Sen, R., Kausel, E., and Banerjee, P.K., 'Dynamic Analysis of Piles and Pile Groups in Non-homogeneous Soils,' Int. Journal of Num. and Anal. Meth. in Geomech., Vol. 9, 1985, pp. 507-524.

22. Wong, H.L. and Luco, J.E., 'Dynamic Response of Rectangular Foundations to Obliquely Incident Seismic Waves,' Journal of Earthq. Eng. and Struct. Dynamics, Vol. 6, 1978.

NATIONAL CENTER FOR EARTHQUAKE ENGINEERING RESEARCH
LIST OF PUBLISHED TECHNICAL REPORTS

The National Center for Earthquake Engineering Research (NCEER) publishes technical reports on a variety of subjects related to earthquake engineering written by authors funded through NCEER. These reports are available from both NCEER's Publications Department and the National Technical Information Service (NTIS). Requests for reports should be directed to the Publications Department, National Center for Earthquake Engineering Research, State University of New York at Buffalo, Red Jacket Quadrangle, Buffalo, New York 14261. Reports can also be requested through NTIS, 5285 Port Royal Road, Springfield, Virginia 22161. NTIS accession numbers are shown in parenthesis, if available.

NCEER-87-0001 "First-Year Program in Research, Education and Technology Transfer," 3/5/87, (PB88-134275/AS).

NCEER-87-0002 "Experimental Evaluation of Instantaneous Optimal Algorithms for Structural Control," by R.C. Lin, T.T. Soong and A.M. Reinhorn, 4/20/87, (PB88-134341/AS).

NCEER-87-0003 "Experimentation Using the Earthquake Simulation Facilities at University at Buffalo," by A.M. Reinhorn and R.L. Ketter, to be published.

NCEER-87-0004 "The System Characteristics and Performance of a Shaking Table," by J.S. Hwang, K.C. Chang and G.C. Lee, 6/1/87, (PB88-134259/AS).

NCEER-87-0005 "A Finite Element Formulation for Nonlinear Viscoplastic Material Using a Q Model," by O. Gyebi and G. Dasgupta, 11/2/87, (PB88-213764/AS).

NCEER-87-0006 "Symbolic Manipulation Program (SMP) - Algebraic Codes for Two and Three Dimensional Finite Element Formulations," by X. Lee and G. Dasgupta, 11/9/87, (PB88-219522/AS).

NCEER-87-0007 "Instantaneous Optimal Control Laws for Tall Buildings Under Seismic Excitations," by J.N. Yang, A. Akbarpour and P. Ghaemmaghami, 6/10/87, (PB88-134333/AS).

NCEER-87-0008 "IDARC: Inelastic Damage Analysis of Reinforced Concrete Frame - Shear-Wall Structures," by Y.J. Park, A.M. Reinhorn and S.K. Kunnath, 7/20/87, (PB88-134325/AS).

NCEER-87-0009 "Liquefaction Potential for New York State: A Preliminary Report on Sites in Manhattan and Buffalo," by M. Budhu, V. Vijayakumar, R.F. Giese and L. Baumgras, 8/31/87, (PB88-163704/AS). This report is available only through NTIS (see address given above).

NCEER-87-0010 "Vertical and Torsional Vibration of Foundations in Inhomogeneous Media," by A.S. Veletsos and K.W. Dotson, 6/1/87, (PB88-134291/AS).

NCEER-87-0011 "Seismic Probabilistic Risk Assessment and Seismic Margins Studies for Nuclear Power Plants," by Howard H.M. Hwang, 6/15/87, (PB88-134267/AS). This report is available only through NTIS (see address given above).

NCEER-87-0012 "Parametric Studies of Frequency Response of Secondary Systems Under Ground-Acceleration Excitations," by Y. Yong and Y.K. Lin, 6/10/87, (PB88-134309/AS).

NCEER-87-0013 "Frequency Response of Secondary Systems Under Seismic Excitation," by J.A. HoLung, J. Cai and Y.K. Lin, 7/31/87, (PB88-134317/AS).

NCEER-87-0014 "Modelling Earthquake Ground Motions in Seismically Active Regions Using Parametric Time Series Methods," by G.W. Ellis and A.S. Cakmak, 8/25/87, (PB88-134283/AS).

NCEER-87-0015 "Detection and Assessment of Seismic Structural Damage," by E. DiPasquale and A.S. Cakmak, 8/25/87, (PB88-163712/AS).

NCEER-87-0016 "Pipeline Experiment at Parkfield, California," by J. Isenberg and E. Richardson, 9/15/87, (PB88-163720/AS).

NCEER-87-0017 "Digital Simulation of Seismic Ground Motion," by M. Shinozuka, G. Deodatis and T. Harada, 8/31/87, (PB88-155197/AS). This report is available only through NTIS (see address given above).

NCEER-87-0018 "Practical Considerations for Structural Control: System Uncertainty, System Time Delay and Truncation of Small Control Forces," J.N. Yang and A. Akbarpour, 8/10/87, (PB88-163738/AS).

NCEER-87-0019 "Modal Analysis of Nonclassically Damped Structural Systems Using Canonical Transformation," by J.N. Yang, S. Sarkani and F.X. Long, 9/27/87, (PB88-187851/AS).

NCEER-87-0020 "A Nonstationary Solution in Random Vibration Theory," by J.R. Red-Horse and P.D. Spanos, 11/3/87, (PB88-163746/AS).

NCEER-87-0021 "Horizontal Impedances for Radially Inhomogeneous Viscoelastic Soil Layers," by A.S. Veletsos and K.W. Dotson, 10/15/87, (PB88-150859/AS).

NCEER-87-0022 "Seismic Damage Assessment of Reinforced Concrete Members," by Y.S. Chung, C. Meyer and M. Shinozuka, 10/9/87, (PB88-150867/AS). This report is available only through NTIS (see address given above).

NCEER-87-0023 "Active Structural Control in Civil Engineering," by T.T. Soong, 11/11/87, (PB88-187778/AS).

NCEER-87-0024 Vertical and Torsional Impedances for Radially Inhomogeneous Viscoelastic Soil Layers," by K.W. Dotson and A.S. Veletsos, 12/87, (PB88-187786/AS).

NCEER-87-0025 "Proceedings from the Symposium on Seismic Hazards, Ground Motions, Soil-Liquefaction and Engineering Practice in Eastern North America," October 20-22, 1987, edited by K.H. Jacob, 12/87, (PB88-188115/AS).

NCEER-87-0026 "Report on the Whittier-Narrows, California, Earthquake of October 1, 1987," by J. Pantelic and A. Reinhorn, 11/87, (PB88-187752/AS). This report is available only through NTIS (see address given above).

NCEER-87-0027 "Design of a Modular Program for Transient Nonlinear Analysis of Large 3-D Building Structures," by S. Srivastav and J.F. Abel, 12/30/87, (PB88-187950/AS).

NCEER-87-0028 "Second-Year Program in Research, Education and Technology Transfer," 3/8/88, (PB88-219480/AS).

NCEER-88-0001 "Workshop on Seismic Computer Analysis and Design of Buildings With Interactive Graphics," by W. McGuire, J.F. Abel and C.H. Conley, 1/18/88, (PB88-187760/AS).

NCEER-88-0002 "Optimal Control of Nonlinear Flexible Structures," by J.N. Yang, F.X. Long and D. Wong, 1/22/88, (PB88-213772/AS).

NCEER-88-0003 "Substructuring Techniques in the Time Domain for Primary-Secondary Structural Systems," by G.D. Manolis and G. Juhn, 2/10/88, (PB88-213780/AS).

NCEER-88-0004 "Iterative Seismic Analysis of Primary-Secondary Systems," by A. Singhal, L.D. Lutes and P.D. Spanos, 2/23/88, (PB88-213798/AS).

NCEER-88-0005 "Stochastic Finite Element Expansion for Random Media," by P.D. Spanos and R. Ghanem, 3/14/88, (PB88-213806/AS).

NCEER-88-0006 "Combining Structural Optimization and Structural Control," by F.Y. Cheng and C.P. Pantelides, 1/10/88, (PB88-213814/AS).

NCEER-88-0007 "Seismic Performance Assessment of Code-Designed Structures," by H.H-M. Hwang, J-W. Jaw and H-J. Shau, 3/20/88, (PB88-219423/AS).

NCEER-88-0008 "Reliability Analysis of Code-Designed Structures Under Natural Hazards," by H.H-M. Hwang, H. Ushiba and M. Shinozuka, 2/29/88, (PB88-229471/AS).

NCEER-88-0009 "Seismic Fragility Analysis of Shear Wall Structures," by J-W Jaw and H.H-M. Hwang, 4/30/88.

NCEER-88-0010 "Base Isolation of a Multi-Story Building Under a Harmonic Ground Motion - A Comparison of Performances of Various Systems," by F-G Fan, G. Ahmadi and I.G. Tadjbakhsh, 5/18/88.

NCEER-88-0011 "Seismic Floor Response Spectra for a Combined System by Green's Functions," by F.M. Lavelle, L.A. Bergman and P.D. Spanos, 5/1/88.

NCEER-88-0012 "A New Solution Technique for Randomly Excited Hysteretic Structures," by G.Q. Cai and Y.K. Lin, 5/16/88.

NCEER-88-0013 "A Study of Radiation Damping and Soil-Structure Interaction Effects in the Centrifuge," by K. Weissman, supervised by J.H. Prevost, 5/24/88.

NCEER-88-0014 "Parameter Identification and Implementation of a Kinematic Plasticity Model for Frictional Soils," by J.H. Prevost and D.V. Griffiths, to be published.

NCEER-88-0015 "Two- and Three- Dimensional Dynamic Finite Element Analyses of the Long Valley Dam," by D.V. Griffiths and J.H. Prevost, 6/17/88.

NCEER-88-0016 "Damage Assessment of Reinforced Concrete Structures in Eastern United States," by A.M. Reinhorn, M.J. Seidel, S.K. Kunnath and Y.J. Park, 6/15/88.

NCEER-88-0017 "Dynamic Compliance of Vertically Loaded Strip Foundations in Multilayered Viscoelastic Soils," by S. Ahmad and A.S.M. Israil, 6/17/88.

NCEER-88-0018 "An Experimental Study of Seismic Structural Response With Added Viscoelastic Dampers," by R.C. Lin, Z. Liang, T.T. Soong and R.H. Zhang, 6/30/88.

NCEER-88-0019 "Experimental Investigation of Primary - Secondary System Interaction," by G.D. Manolis, G. Juhn and A.M. Reinhorn, 5/27/88.

NCEER-88-0020 "A Response Spectrum Approach For Analysis of Nonclassically Damped Structures," by J.N. Yang, S. Sarkani and F.X. Long, 4/22/88.

NCEER-88-0021 "Seismic Interaction of Structures and Soils: Stochastic Approach," by A.S. Veletsos and A.M. Prasad, 7/21/88.

NCEER-88-0022 "Identification of the Serviceability Limit State and Detection of Seismic Structural Damage," by E. DiPasquale and A.S. Cakmak, 6/15/88.

NCEER-88-0023 "Multi-Hazard Risk Analysis: Case of a Simple Offshore Structure," by B.K. Bhartia and E.H. Vanmarcke, 7/21/88.

NCEER-88-0024 "Automated Seismic Design of Reinforced Concrete Buildings," by Y.S. Chung, C. Meyer and M. Shinozuka, 7/5/88.

NCEER-88-0025 "Experimental Study of Active Control of MDOF Structures Under Seismic Excitations," by L.L. Chung, R.C. Lin, T.T. Soong and A.M. Reinhorn, 7/10/88.

NCEER-88-0026 "Earthquake Simulation Tests of a Low-Rise Metal Structure," by J.S. Hwang, K.C. Chang, G.C. Lee and R.L. Ketter, 8/1/88.

NCEER-88-0027 "Systems Study of Urban Response and Reconstruction Due to Catastrophic Earthquakes," by F. Kozin and H.K. Zhou, 9/22/88, to be published.

NCEER-88-0028 "Seismic Fragility Analysis of Plane Frame Structures," by H.H-M. Hwang and Y.K. Low, 7/31/88.

NCEER-88-0029 "Response Analysis of Stochastic Structures," by A. Kardara, C. Bucher and M. Shinozuka, 9/22/88, to be published.

NCEER-88-0030 "Nonnormal Accelerations Due to Yielding in a Primary Structure," by D.C.K. Chen and L.D. Lutes, 9/19/88.

NCEER-88-0031 "Design Approaches for Soil-Structure Interaction," by A.S. Veletsos, A.M. Prasad and Y. Tang, to be published.

NCEER-88-0032 "A Re-evaluation of Design Spectra for Seismic Damage Control," by C.J. Turkstra and A.G. Tallin, 11/7/88.

NCEER-88-0033 "The Behavior and Design of Noncontact Lap Splices Subjected to Repeated Inelastic Tensile Loading," by V.E. Sagan, P. Gergely and R.N. White, to be published.

NCEER-88-0034 "Seismic Response of Pile Foundations," by S.M. Mamoon, P.K. Banerjee and S. Ahmad, 11/1/88.